

2. FINITE ELEMENT ANALYSIS

2.1 INTRODUCTION

To predict the complicated behavior of double angle web connections, a 3D nonlinear finite element model for half of the entire connection is generated using the ABAQUS finite element software package. Double angle connections are modeled to investigate the effect of angle thickness, t , on the load-displacement relationship and the moment-rotation relationship under axial tensile loads, shear loads, and combined axial tensile loads plus shear loads. Three angle sections, L5x3x1/4, L5x3x3/8, and L5x3x1/2, were selected for this purpose. The same gage distance, g , bolt spacing, s , and bolt diameter are used for these three cases; A36 steel is used for the three angles.

2.2 FINITE ELEMENT 3D ANALYSIS

One-half of an entire double angle web connection is modeled using the following ABAQUS element types:

- i) C3D20 (20-node quadratic brick) element types are used for the angle specimens and bolts. Hex bolt heads and nuts are idealized as square bolt heads and nuts to simplify the analysis. Washers are not modeled in this analysis.
- ii) C3D8 (8-node linear brick) element types are used for the beam. The entire beam model is simplified as a beam web having the same moment of inertia as that of an actual beam with respect to the strong axis.
- iii) C3D6 (6-node linear triangular prism) element types are used for the welds.

iv) SPRING2 (spring between two nodes, acting in a fixed direction) element types are used to simulate the column. A spring stiffness of 2×10^3 is used for the simulation of a column resisting compression forces, while a spring stiffness of 5×10^{-12} is used for the simulation of interactions between a column and an angle under tension forces.

The first two of these element types are represented in Figure 2.1.

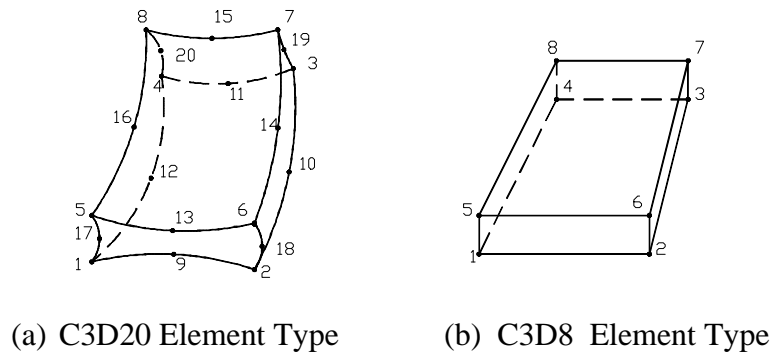
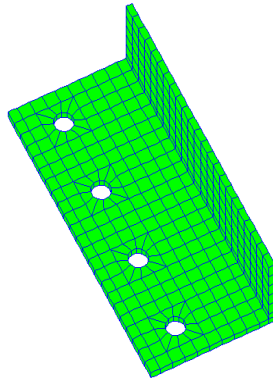


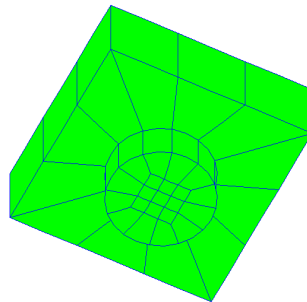
Figure 2.1 ABAQUS Element Types

The ABAQUS “*CONTACT PAIR, SMALL SLIDING” option and “*SURFACE BEHAVIOR, NO SEPARATION” option are used to simulate the contact problems between bolt heads and outstanding legs of angles. The contact and bearing problems between bolt shanks and bolt holes are neglected due to computer time and cost required for such an analysis. The “*MPC (Multi-Point Constraints)” option is used to impose constraints between a beam element and a back-to-back angle leg of each angle. Prestressing forces are applied to each bolt as initial stresses to simulate the fully-tightened bolts with minimum bolt tension. For this procedure, the “*BOUNDARY,

OP=NEW, FIXED” option and “*CLOAD, OP=NEW” option are used to apply 28 kips to each bolt as the prestress force. Elastic-perfectly plastic material behavior is considered for each element and the von Mises yield criterion is used to represent the yielding of steel in this analysis. Figure 2.2 shows an angle model and a bolt model used in the 3D finite element analysis. Each entire 3D finite element model consists of an angle, four bolts, springs, and a beam.



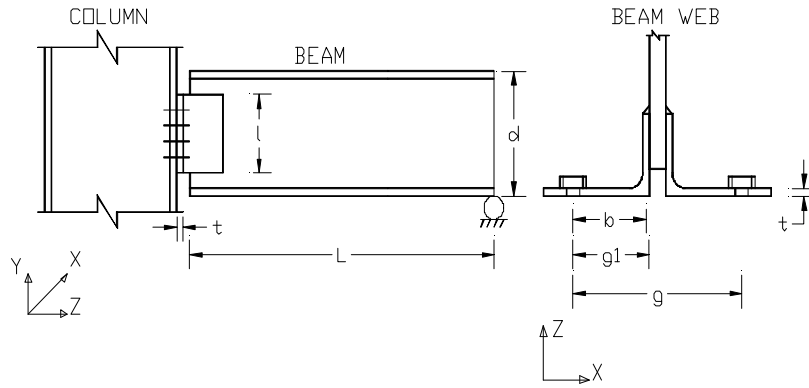
(a) Angle Model



(b) Bolt Model

Figure 2.2 ABAQUS Finite Element Model

Three angle sections, L5x3x1/4, L5x3x3/8, and L5x3x1/2, were studied to predict the load-displacement relationship under axial loadings and the moment-rotation relationship under shear loadings and axial loadings plus shear loadings. Each angle specimen is connected to a W18x35 beam and a W14x90 column with 3/4 in. diameter A325-N bolts and 3/16 in. E70xx welds. The bolt spacing is 3 in. center-to-center of the bolts. Figure 2.3 shows the details of the double angle connections studied.

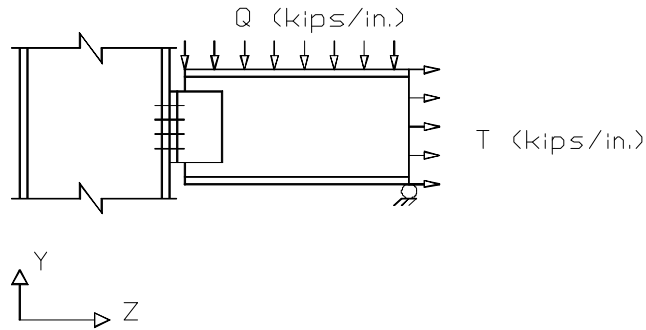


	t (in.)	d (in.)	L (in.)	g (in.)	$g1=(g-t,beam)/2$ (in.)	$b=(g1-(t,angle/2))$ (in.)
L5x3x1/4 Angle	0.25	17.7	240	7.5	3.6	3.475
L5x3x3/8 Angle	0.375	17.7	240	7.5	3.6	3.4125
L5x3x1/2 Angle	0.5	17.7	240	7.5	3.6	3.35

Figure 2.3 Geometric Parameters of the Double Angle Connections

For the entire 3D finite element model with an L5x3x1/4 angle, 1,330 elements, which have 6,136 nodes, were used. The total number of variables (degrees of freedom plus any Lagrange multiplier variables) in the model is equal to 16,644. For the entire 3D finite element model with an L5x3x3/8 angle, the same number of elements, nodes, and variables is used. For the entire 3D finite element model with an L5x3x1/2 angle, 1,305 elements, which have 5,956 nodes, are used. The total number of variables in this model is 16,128.

Figure 2.4 defines the loading conditions for each case used in the ABAQUS executions, and the reference displacement and angle change under each loading condition. The ABAQUS executions were terminated when the displacement of the corner of an angle exceeded 0.5 in.



	Maximum Values of Q (kips/in.)	Maximum Values of T (kips/in.)
L5x3x1/4 Angle Under Axial Loading	0	1.13
L5x3x1/4 Angle Under Shear Loading	0.3334	0
L5x3x1/4 Angle Under Axial Loading Plus Shear Loading	0.3334	1.13
L5x3x3/8 Angle Under Axial Loading	0	2.26
L5x3x3/8 Angle Under Shear Loading	0.3334	0
L5x3x3/8 Angle Under Axial Loading Plus Shear Loading	0.3334	2.26
L5x3x1/2 Angle Under Axial Loading	0	2.26
L5x3x1/2 Angle Under Shear Loading	0.3334	0
L5x3x1/2 Angle Under Axial Loading Plus Shear Loading	0.3334	2.26

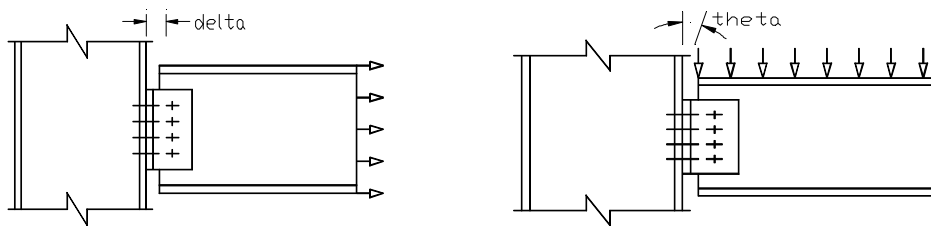


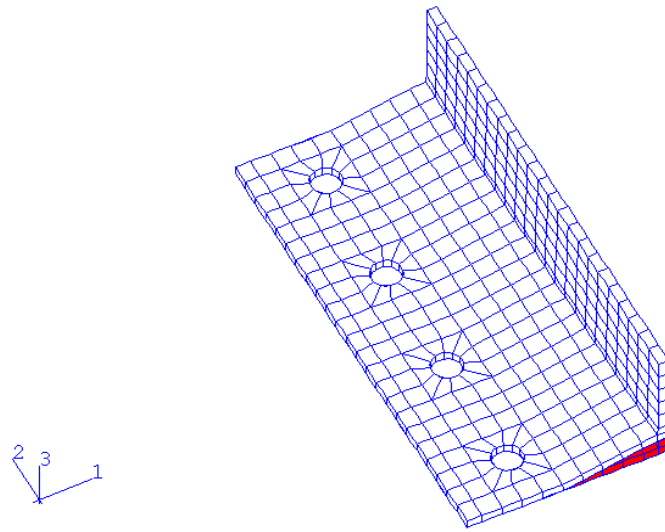
Figure 2.4 Loading Conditions and Measurements of Displacement and Angle Change

2.2.1 L5x3x1/4 Angle Model

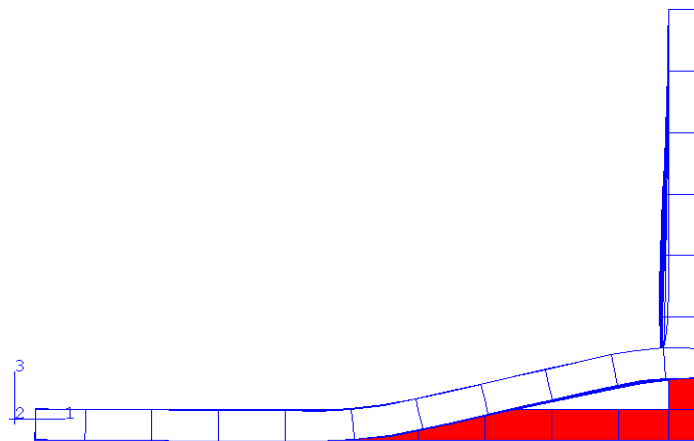
2.2.1.1 Angle Under Axial Tensile Loading

To establish the load-displacement relationship of an L5x3x1/4 double angle connection, increasing axial tensile loads are applied to the end of beam elements in the positive Z-direction. Then, the load-displacement relationship is obtained by determining

the variations of the displacement of the corner of the angle with the applied tensile loads at each loading stage. Figure 2.5 depicts a deformed shape of the angle connection at the final loading stage (total of 12.0 kips to the end of the beam). The angle and beam elements have been uniformly pulled up in the positive Z-direction. Figure 2.6 presents the load-displacement relationship of an L5x3x1/4 double angle connection that has been subjected to an axial tensile load that is increased until the displacement reaches 0.5 in. The load-displacement curve shows a linear relationship initially, followed by a gradual decrease in stiffness. The initial stiffness of this angle model is 116.7 kips/in., while the final stiffness is approximately 8.6 kips/in. Table 2.1 summarizes the above load-displacement relationship at each loading stage.



(a) Deformed Shape of an Angle Model



(b) Side View of a Deformed Angle Model

Figure 2.5 Deformed Shape of an L5x3x1/4 Double Angle Connection
due to Tension Loading

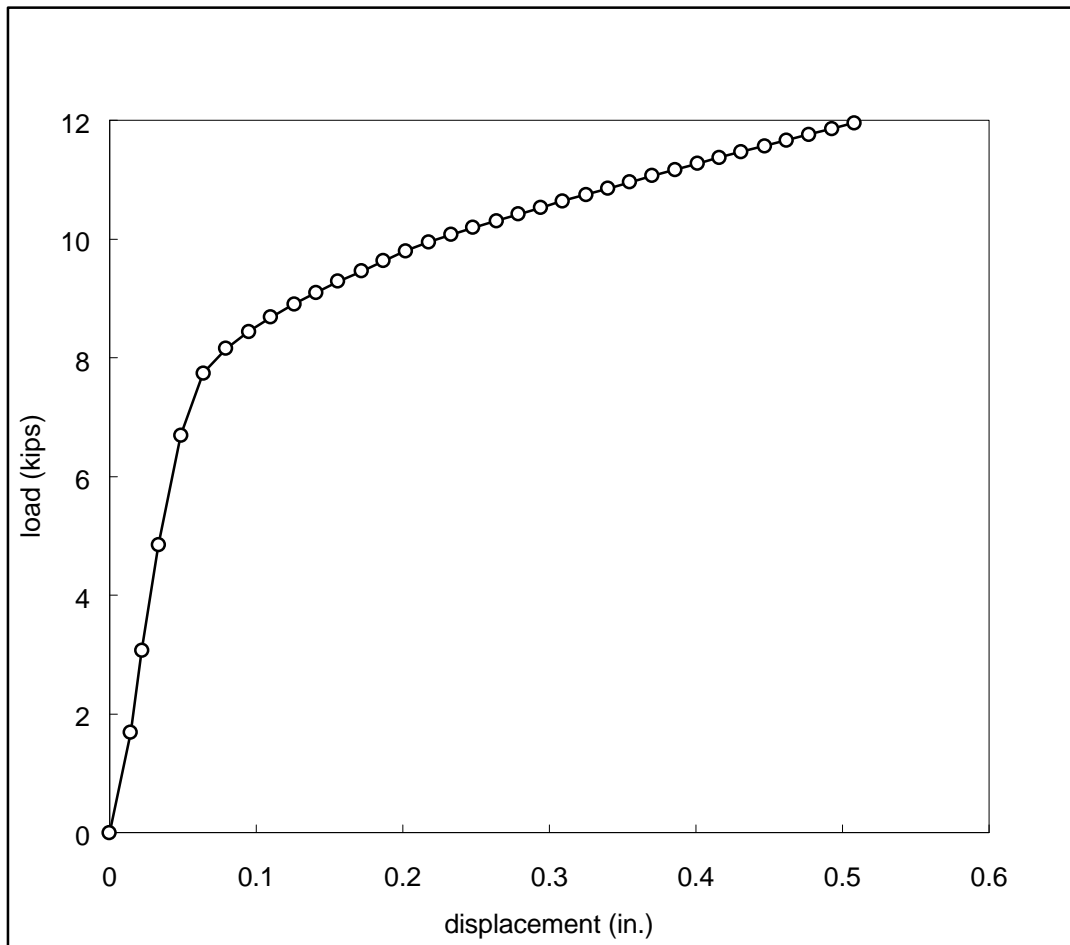


Figure 2.6 Load-Displacement Relationship for an L5x3x1/4 Double Angle Connection due to Tension Loading

Table 2.1 Data for the Load-Displacement Relationship of an L5x3x1/4 Double Angle

Connection due to Tension Loading

Loading Stage	Displacement (in.)	Load (kips)
1	0	0
2	0.0145	1.692
3	0.0221	3.073
4	0.0335	4.844
5	0.0487	6.695
6	0.064	7.741
7	0.0795	8.158
8	0.0949	8.444
9	0.11	8.686
10	0.126	8.903
11	0.141	9.101
12	0.156	9.287
13	0.172	9.463
14	0.187	9.634
15	0.202	9.798
16	0.218	9.95
17	0.233	10.075
18	0.248	10.195
19	0.264	10.309
20	0.279	10.421
21	0.294	10.53
22	0.309	10.639
23	0.325	10.747
24	0.34	10.854
25	0.355	10.961
26	0.37	11.065
27	0.386	11.17
28	0.401	11.272
29	0.416	11.372
30	0.431	11.472
31	0.447	11.57
32	0.462	11.668
33	0.477	11.765
34	0.493	11.861
35	0.508	11.957

Figure 2.7 shows the von Mises stress diagram of an L5x3x1/4 angle specimen at the final loading stage. Yielding zones are observed in the outstanding leg of the angle near the bolt heads and close to the corner of the angle. These yielding zones are propagated toward the centers of the bolt holes as the applied loads increase.

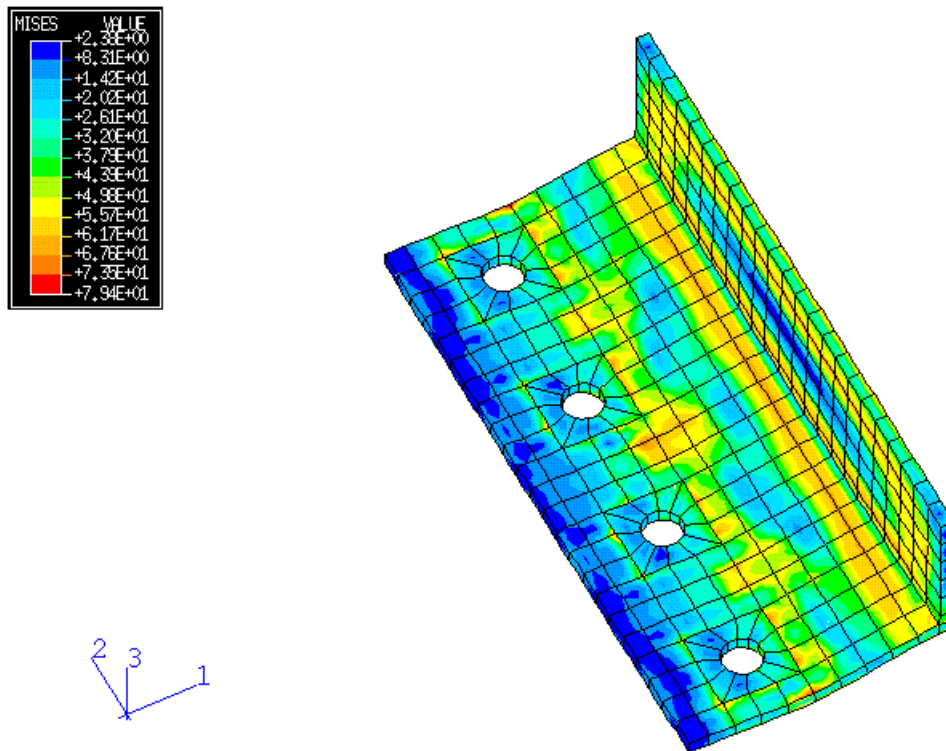


Figure 2.7 von Mises Stress Diagram of an L5x3x1/4 Angle due to Tension Loading

Figure 2.8 shows the tension bolt force-applied load relationship for the L5x3x1/4 double angle connection. At an applied load of 1.69 kips, the sum of the bolt forces is 2.47 kips. The outer bolts (bolt 1 and bolt 4) show approximately the same amount of bolt force at each loading stage. Similarly, the inner bolts (bolt 2 and bolt 3) show the same symmetric behavior as that of the outer bolts under the applied loads. Beyond the applied load of 7.74 kips in Figure 2.8, the sum of bolt forces in the Z-direction shows rapid increases.

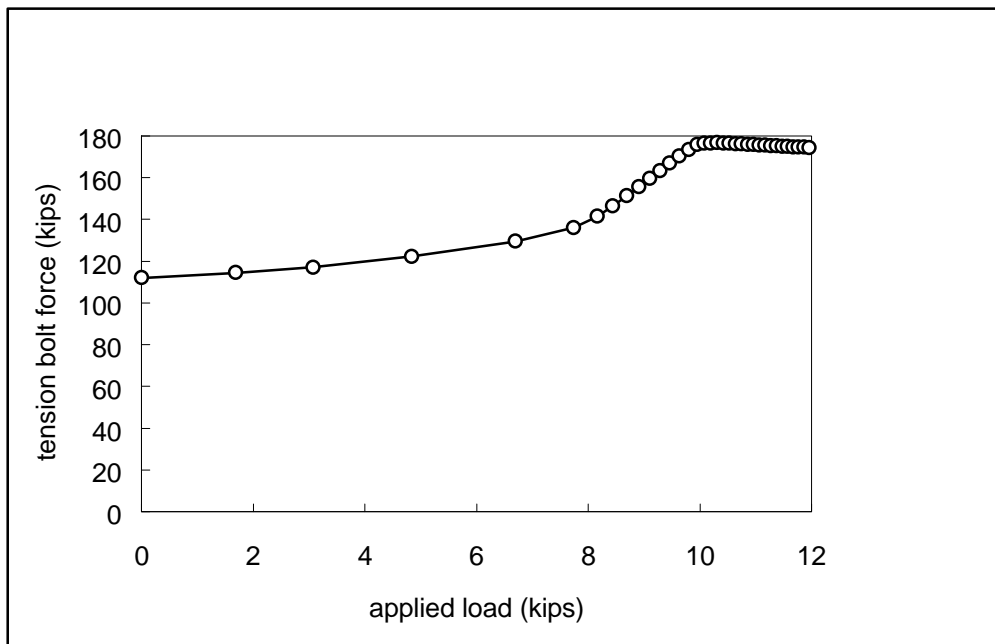


Figure 2.8 Tension Bolt Force vs. Applied Load Relationship for the L5x3x1/4 Double Angle Connection

Figure 2.9 shows the von Mises stress diagram of each bolt element at the final loading stage. Fields of high stress are observed in each bolt near the inner edge of the bolt head and the outer edge of the bolt shank. These stress fields propagate as the applied loads increase.

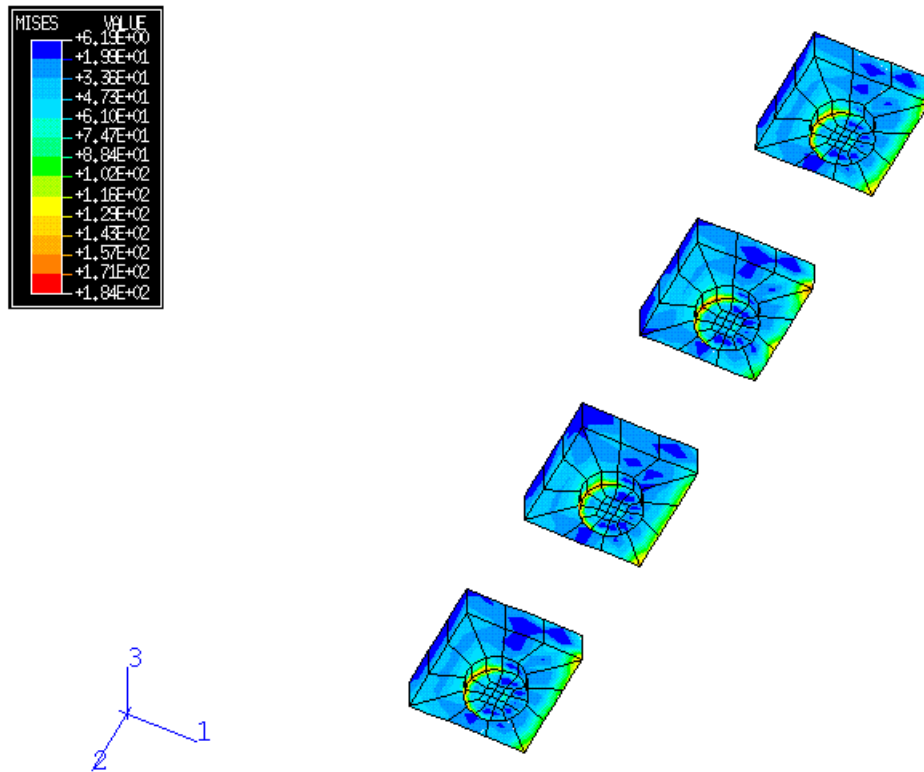


Figure 2.9 von Mises Stress Diagram of Each Bolt used for the L5x3x1/4
Double Angle Connection

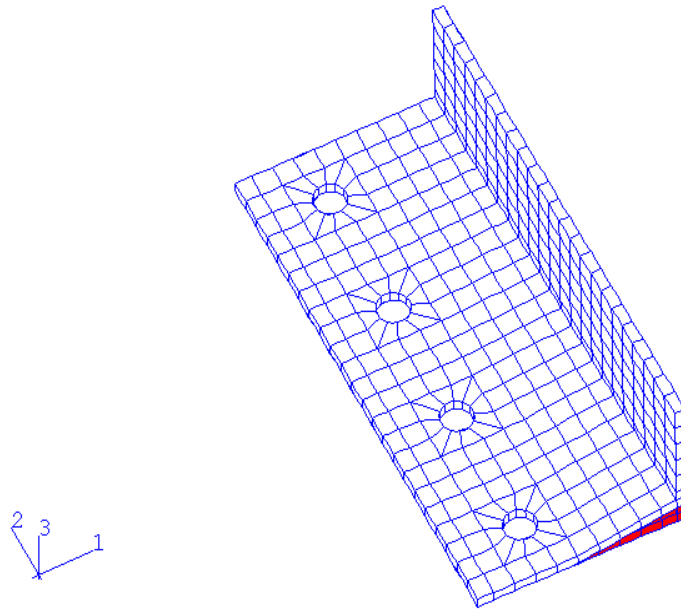
Table 2.2 shows the data for the tension bolt force-applied load relationship as described before.

Table 2.2 Data for the Tension Bolt Force vs. Applied Load Relationship of the L5x3x1/4 Double Angle Connection

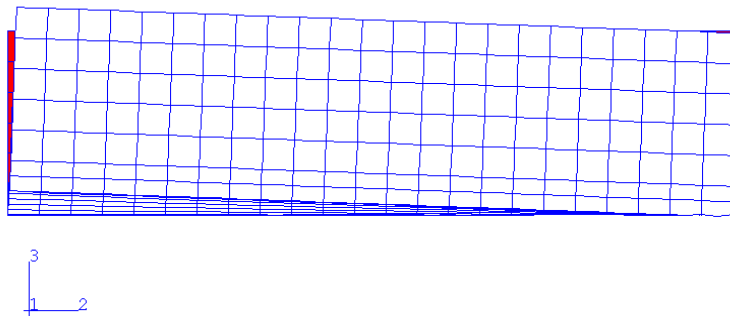
Loading Stage	Applied Load (kips)	Total Bolt Forces (kips)
1	0	112
2	1.69	114.47
3	3.07	117.11
4	4.84	122.21
5	6.70	129.49
6	7.74	136.02
7	8.16	141.45
8	8.44	146.46
9	8.69	151.14
10	8.90	155.50
11	9.10	159.57
12	9.29	163.36
13	9.46	166.91
14	9.63	170.34
15	9.80	173.32
16	9.95	175.70
17	10.08	176.26
18	10.20	176.54
19	10.31	176.57
20	10.42	176.53
21	10.53	176.37
22	10.64	176.21
23	10.75	176.05
24	10.85	175.89
25	10.96	175.73
26	11.07	175.58
27	11.17	175.43
28	11.27	175.28
29	11.37	175.13
30	11.47	174.99
31	11.57	174.85
32	11.67	174.70
33	11.77	174.56
34	11.86	174.42
35	11.96	174.28

2.2.1.2 Angle Under Shear Loading

An increasing, uniformly distributed load is applied to the beam in the negative Y-direction (downward) as shown in Figure 2.4 to investigate the moment-rotation relationship. The moment-rotation relationship of an L5x3x1/4 double angle connection can be established by determining the rotational angle change, ϕ , along with the connection moment, M , at each loading stage. The connection moment, M , can be obtained by a simple static procedure. Figure 2.10 shows the deformed shape of the angle connection under the applied load of 0.3334 kips/in. (total 80 kips). Under the uniformly distributed load, the top of the angle element moves in the Z-direction, while the bottom of the angle element remains in the same position, restrained by the spring elements. Figure 2.11 presents the moment-rotation relationship of the L5x3x1/4 double angle connection. The moment-rotation curve shows almost a linear relationship after the second loading stage (at the applied load of 2 kips) and flattens out gradually as the moment increases. The initial rotational stiffness of the angle connection is approximately 3,559 in.-kips/rad. Table 2.3 contains the data for this moment-rotation relationship of an L5x3x1/4 double angle connection.



(a) Deformed Shape of an Angle Model



(b) Side View of a Back-to-Back Angle Leg

Figure 2.10 Deformed Shape of an L5x3x1/4 Double Angle Connection
due to Shear Loading

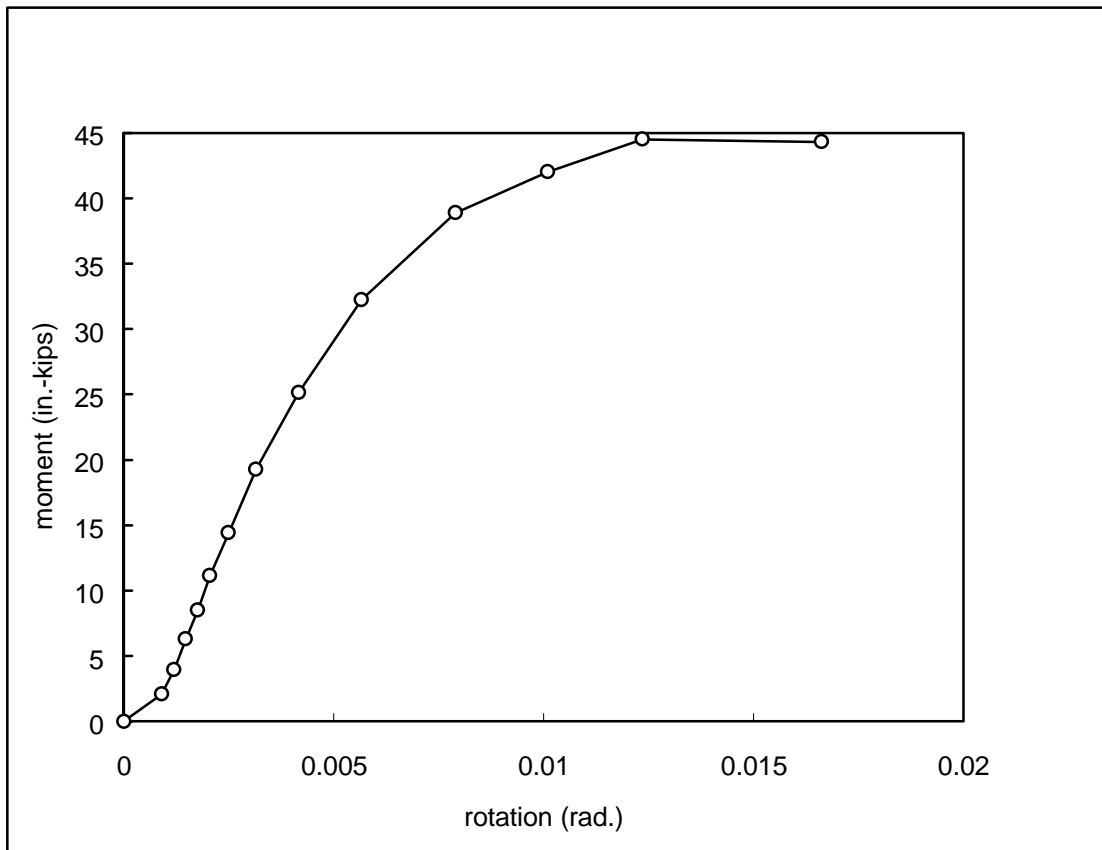


Figure 2.11 Moment-Rotation Relationship of an L5x3x1/4 Double Angle Connection due to Shear Loading

Table 2.3 Data for the Moment-Rotation Relationship of an L5x3x1/4

Double Angle Connection due to Shear Loading

Loading Stage	Applied Load (kips)	Rotation (rad.)	Moment (in.-kips)
1	0	0	0
2	2	0.0009	2.087
3	4	0.0012	3.970
4	5.14	0.0015	6.289
5	6.27	0.0018	8.513
6	7.4	0.0021	11.163
7	9.1	0.0025	14.424
8	11.63	0.0032	19.279
9	15.39	0.0042	25.121
10	21.01	0.0057	32.256
11	29.36	0.0079	38.893
12	37.63	0.0101	42.020
13	45.87	0.0124	44.513

Figure 2.12 shows the von Mises stress diagram of an L5x3x1/4 angle at the applied load of 80.1 kips. Like the yielding zones described in previous research (Chen and Lui 1991), the stress fields show the same characteristic aspects. The yielding zones are formed along the corner of the angle in addition to the top areas of the angle. The bottom areas of Figure 2.12 are the top areas of the angle.

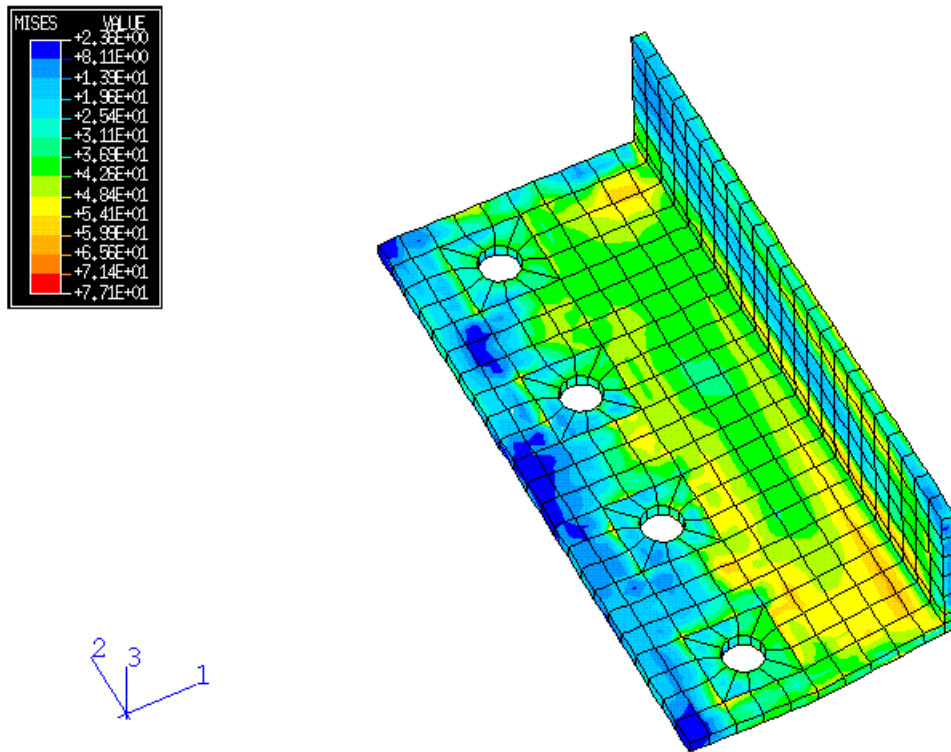


Figure 2.12 von Mises Stress Diagram of an L5x3x1/4 Angle due to Shear Loading

Figure 2.13 presents the von Mises stress diagram of each bolt at the final loading stage. Yielding zones are not formed in the same ways in each bolt indicating that the top areas of the angle are under tension, while the bottom areas of the angle are in compression.

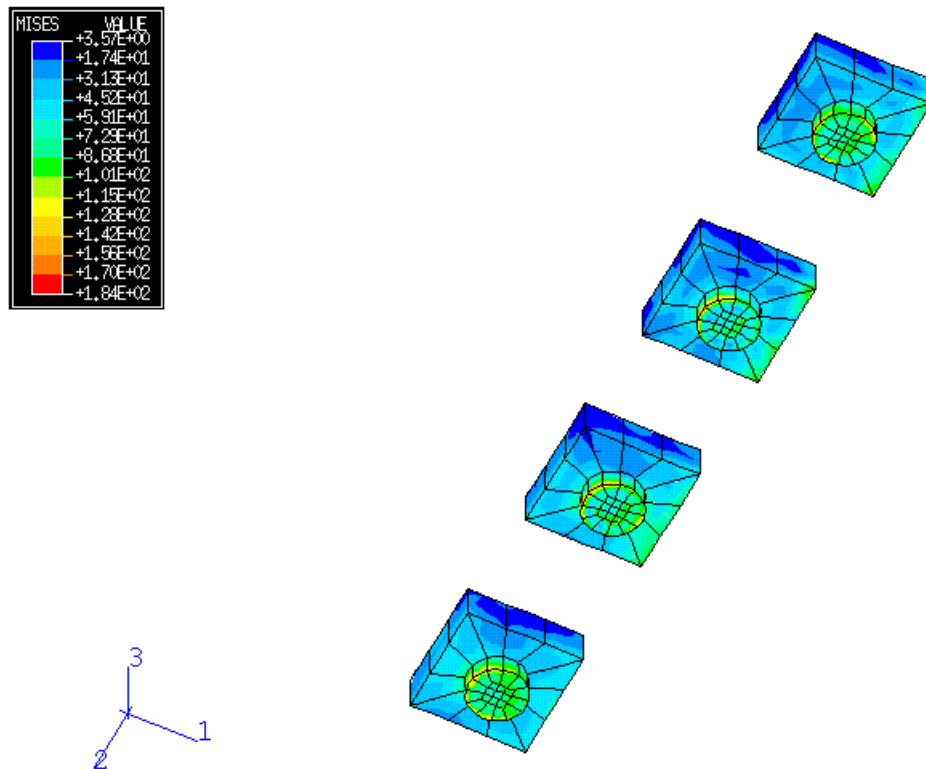
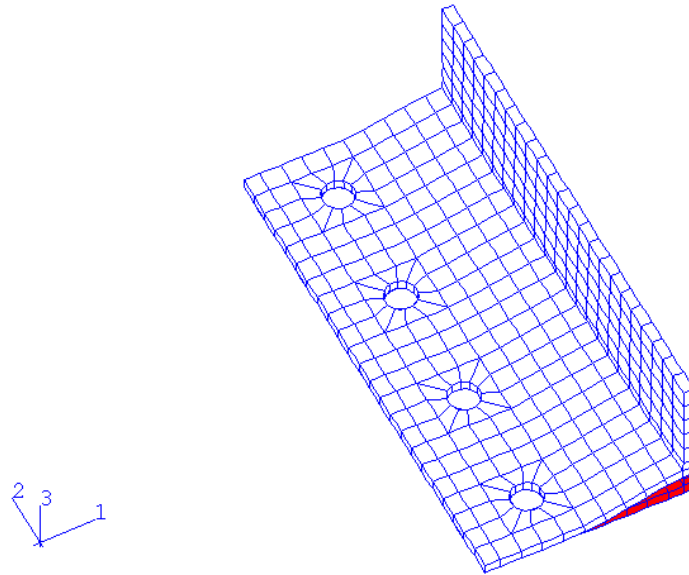


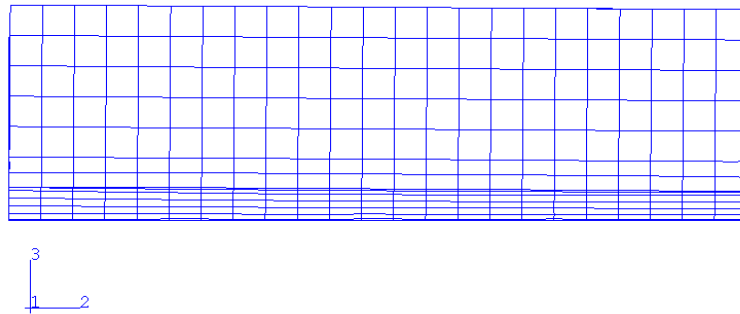
Figure 2.13 von Mises Stress Diagram of Each Bolt used for the L5x3x1/4
Double Angle Connection

2.2.1.3 Angle Under Axial Tensile Loading Plus Shear Loading

An increasing uniformly distributed load and an increasing axial tensile load are applied to the beam as shown in Figure 2.4 to investigate the moment-rotation relationship. Figure 2.14 shows the deformed shape of the angle connection under the applied shear load of 0.0984 kips/in. (total 23.6 kips) plus the applied axial tensile load of 0.6673 kips/in. (total 11.8 kips). Under the uniformly distributed load plus the axial tensile load, the top of the angle moves farther in the Z-direction than the bottom of the angle. Figure 2.15 presents the moment-rotation relationship of the L5x3x1/4 double angle connection. The moment-rotation relationship curve shows a linear relationship initially. The initial rotational stiffness of the angle connection is approximately 2,775 in.-kips/rad. Table 2.4 contains the data for this moment-rotation relationship of an L5x3x1/4 double angle connection under axial tensile loads plus shear loads.



(a) Deformed Shape of an Angle Model



(b) Side View of a Back-to-Back Angle Leg

Figure 2.14 Deformed Shape of an L5x3x1/4 Double Angle Connection
due to Axial Tensile Loading plus Shear Loading

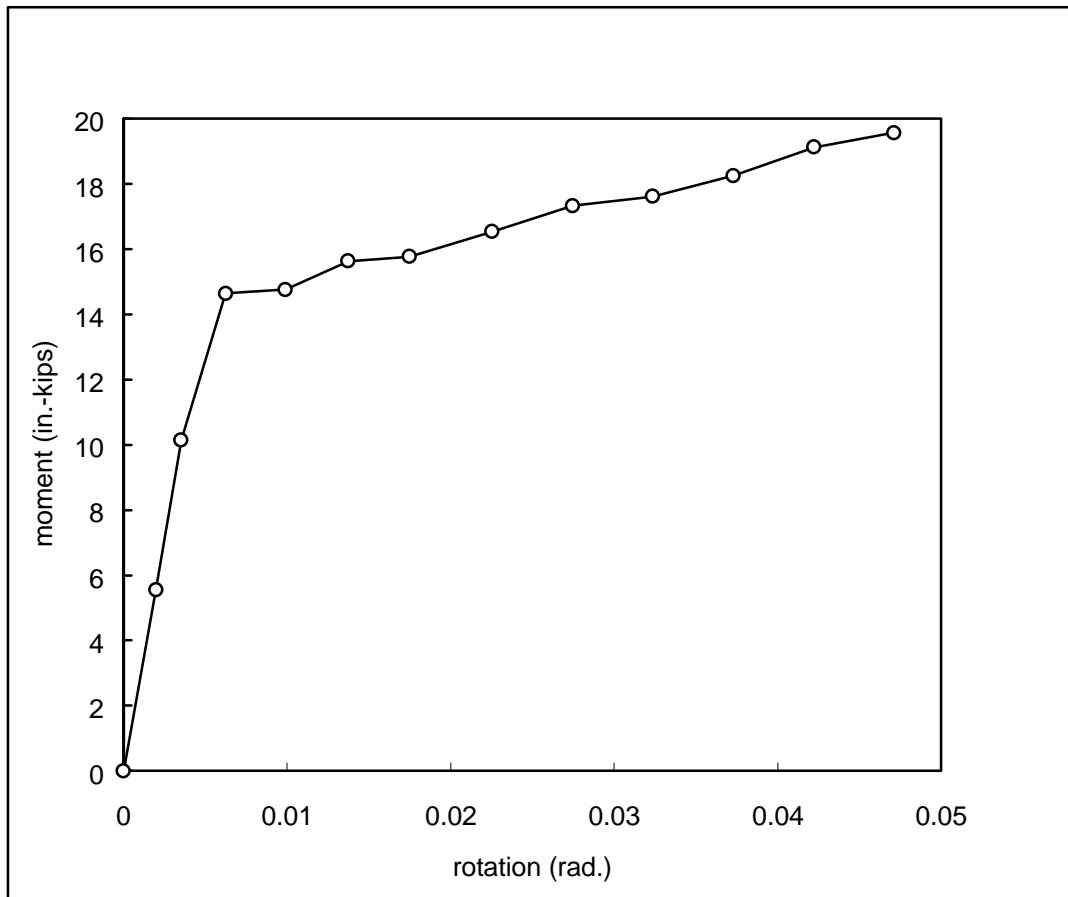


Figure 2.15 Moment-Rotation Relationship of an L5x3x1/4 Double Angle Connection
due to Shear Loading plus Axial Tensile Loading

Table 2.4 Data for the Moment-Rotation Relationship of an L5x3x1/4 Double Angle
 Connection due to Shear Loading plus Axial Tensile Loading

Loading Stage	Q (kips/in.)	T (kips/in.)	Rotation (rad.)	Moment (in.-kips)
1	0	0	0	0
2	0.0163	0.1105	0.0020	5.55
3	0.0320	0.2172	0.0035	10.15
4	0.0540	0.3658	0.0062	14.64
5	0.0681	0.4614	0.0099	14.76
6	0.0737	0.4995	0.0137	15.63
7	0.0780	0.5289	0.0175	15.77
8	0.0828	0.5612	0.0225	16.53
9	0.0864	0.5854	0.0275	17.33
10	0.0896	0.6073	0.0323	17.62
11	0.0926	0.6279	0.0373	18.26
12	0.0956	0.6478	0.0422	19.13
13	0.0984	0.6673	0.0471	19.57

Figure 2.16 shows the von Mises stress diagram of an L5x3x1/4 angle at the applied shear load of 0.0984 kips/in. (total 23.6 kips) plus the applied axial tensile load of 0.6673 kips/in. (total 11.8 kips). Yielding zones are formed in the outstanding leg of the angle near the bolt head and close to the corner of the angle.

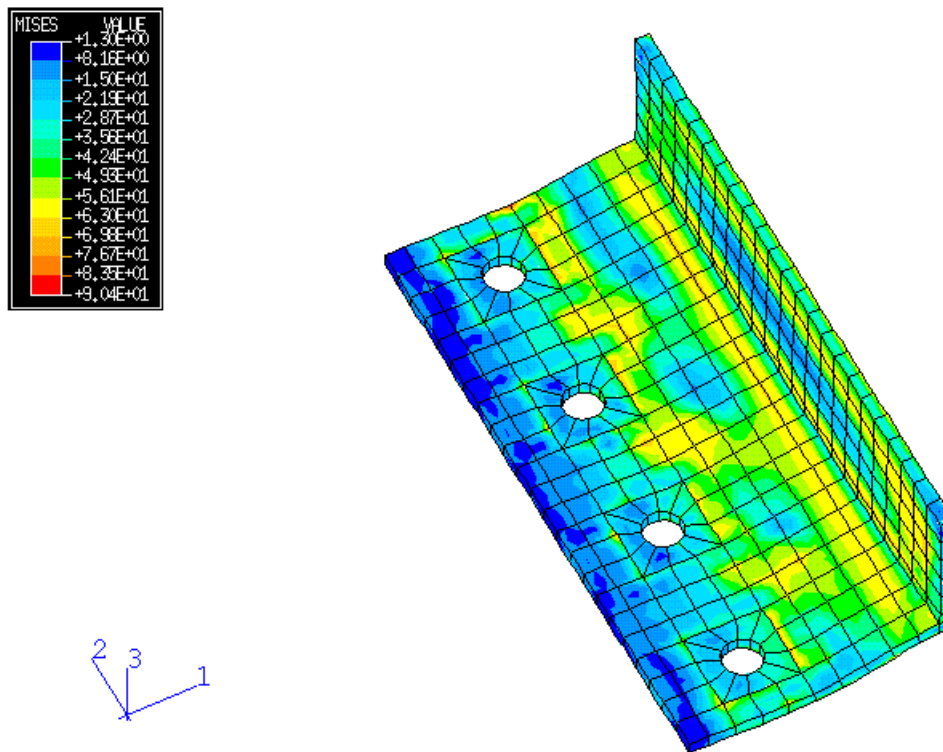
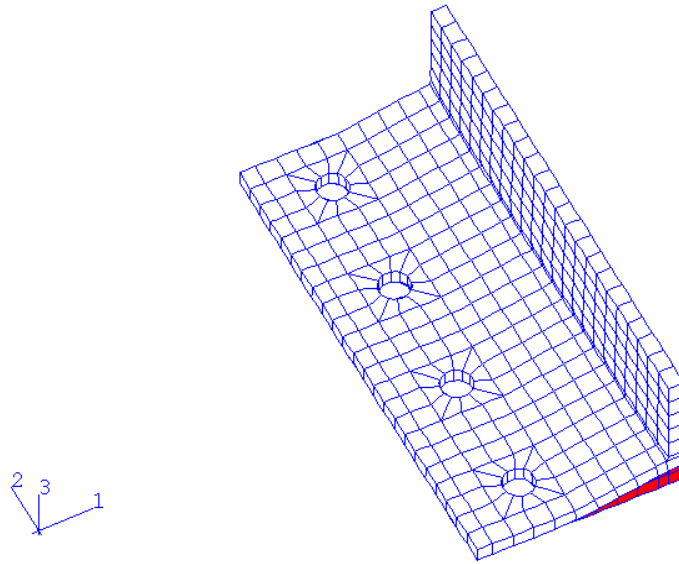


Figure 2.16 von Mises Stress Diagram of an L5x3x1/4 Angle due to Shear Loading plus Axial Tensile Loading

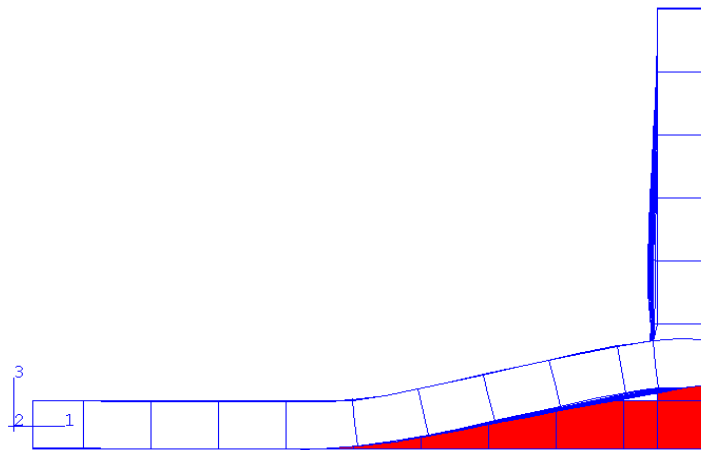
2.2.2 L5x3x3/8 Angle Model

2.2.2.1 Angle Under Axial Tensile Loading

The load-displacement relationship of this angle model was obtained by increasing the load to 2.26 kips/in. (total 40 kips) at one end of the beam in the positive Z-direction. Figure 2.17 depicts the deformed shape of the angle connection at the applied load of 24.3 kips. Figure 2.18 presents the load-displacement relationship of an L5x3x3/8 double angle connection. The load-displacement curve shows a linear relationship initially, followed by a gradual decrease in stiffness like the previous load-displacement relationship for the L5x3x1/4 angle model. The initial stiffness of the angle model is 477.5 kips/in., while the final stiffness is approximately 9.2 kips/in. Table 2.5 contains the above load-displacement relationship at each loading stage.



(a) Deformed Shape of an Angle Model



(b) Side View of a Deformed Angle Model

Figure 2.17 Deformed Shape of an L5x3x3/8 Double Angle Connection
due to Tension Loading

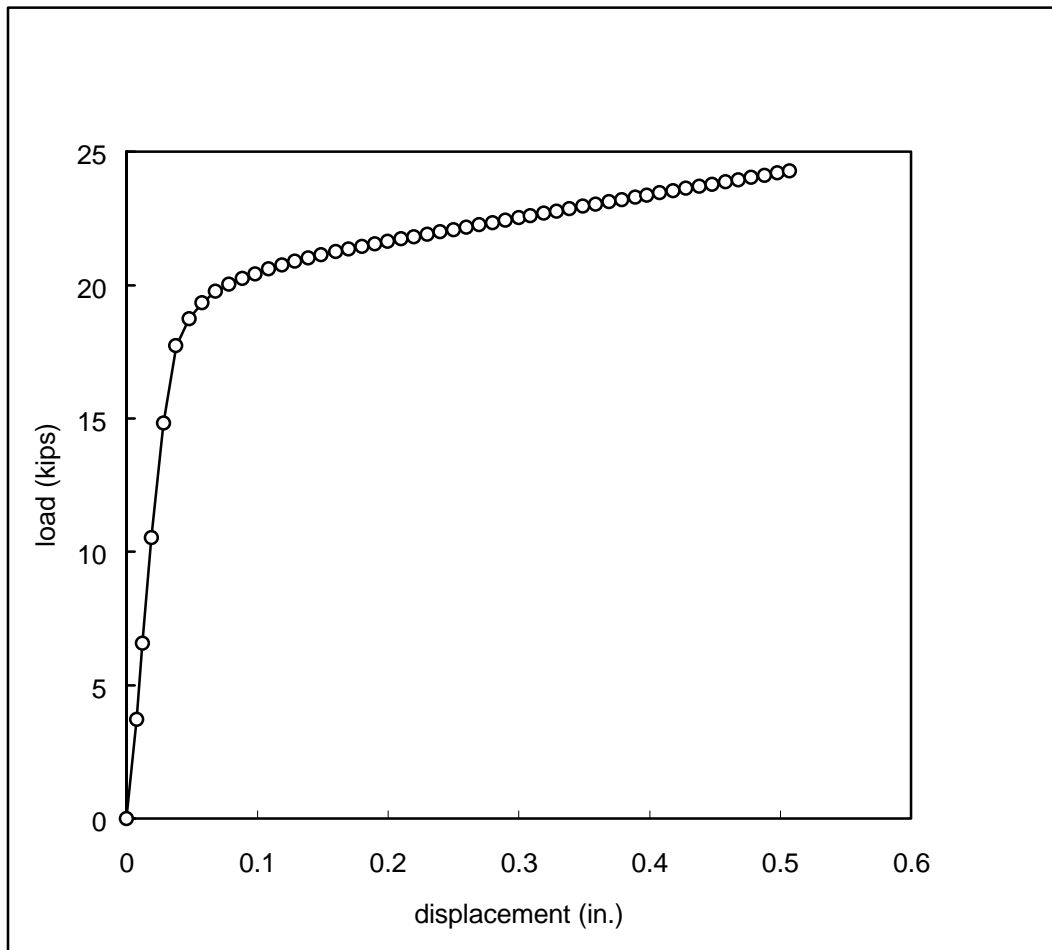


Figure 2.18 Load-Displacement Relationship of an L5x3x3/8 Double Angle Connection due to Tension Loading

Table 2.5 Data for the Load-Displacement Relationship of an L5x3x3/8

Double Angle Connection due to Tension Loading

Loading Stage	Displacement (in.)	Load (kips)
1	0	0
2	0.00778	3.715
3	0.0123	6.58
4	0.0191	10.536
5	0.0284	14.832
6	0.0379	17.724
7	0.0479	18.744
8	0.058	19.332
9	0.0682	19.764
10	0.0784	20.028
11	0.0885	20.232
12	0.0986	20.412
13	0.109	20.592
14	0.119	20.736
15	0.129	20.892
16	0.139	21.012
17	0.149	21.132
18	0.16	21.24
19	0.17	21.348
20	0.18	21.432
21	0.19	21.528
22	0.2	21.624
23	0.21	21.72
24	0.22	21.804
25	0.23	21.888
26	0.24	21.984
27	0.25	22.068
28	0.26	22.152
29	0.27	22.248
30	0.28	22.332
31	0.29	22.416
32	0.3	22.512
33	0.309	22.596
34	0.319	22.68
35	0.329	22.764
36	0.339	22.86
37	0.349	22.944
38	0.359	23.028
39	0.369	23.112
40	0.379	23.196

Figure 2.19 shows the von Mises stress diagram of the angle specimen at the final loading stage. Yielding zones are formed in the outstanding leg of the angle near the bolt heads and close to the corner of the angle like the previous L5x3x1/4 angle model. However, the stress fields are more widely propagated than those of the previous L5x3x1/4 angle model.

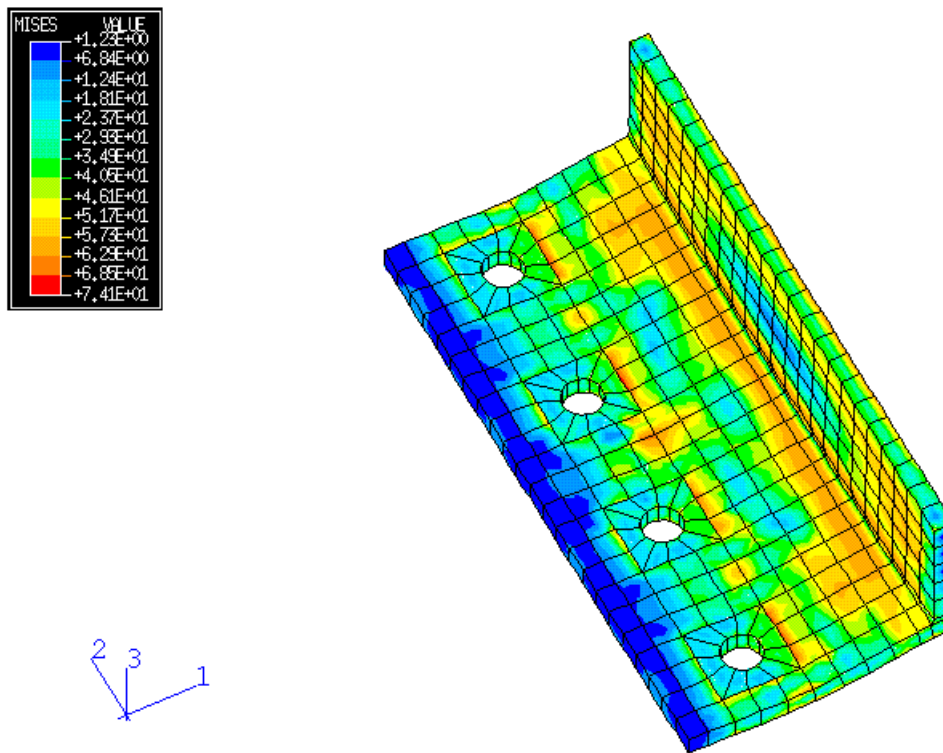


Figure 2.19 von Mises Stress Diagram of an L5x3x3/8 Angle

Figure 2.20 shows the tension bolt force-applied load relationship for the L5x3x3/8 double angle connection. At the applied load of 3.72 kips, the sum of the bolt forces is 2.97 kips. The applied load-bolt force curve increases more gradually than that of the previous L5x3x1/4 angle model. From the applied load of 17.72 kips, the sum of the bolt forces in the Z-direction shows a rapid increase.

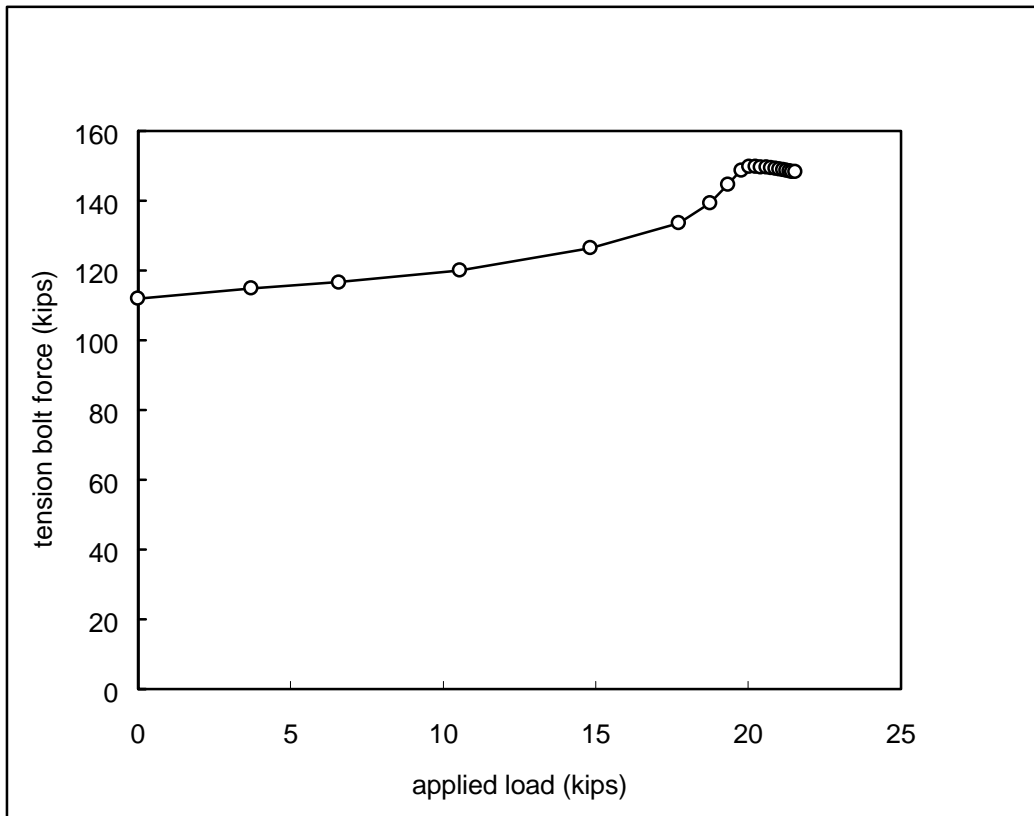


Figure 2.20 Tension Bolt Force vs. Applied Load Relationship for the L5x3x3/8 Double Angle Connection

Figure 2.21 shows the von Mises stress diagram of each bolt element at the final loading stage. Fields of high stress are formed in each bolt near the inner edge of the bolt head and outer edge of the bolt shank.

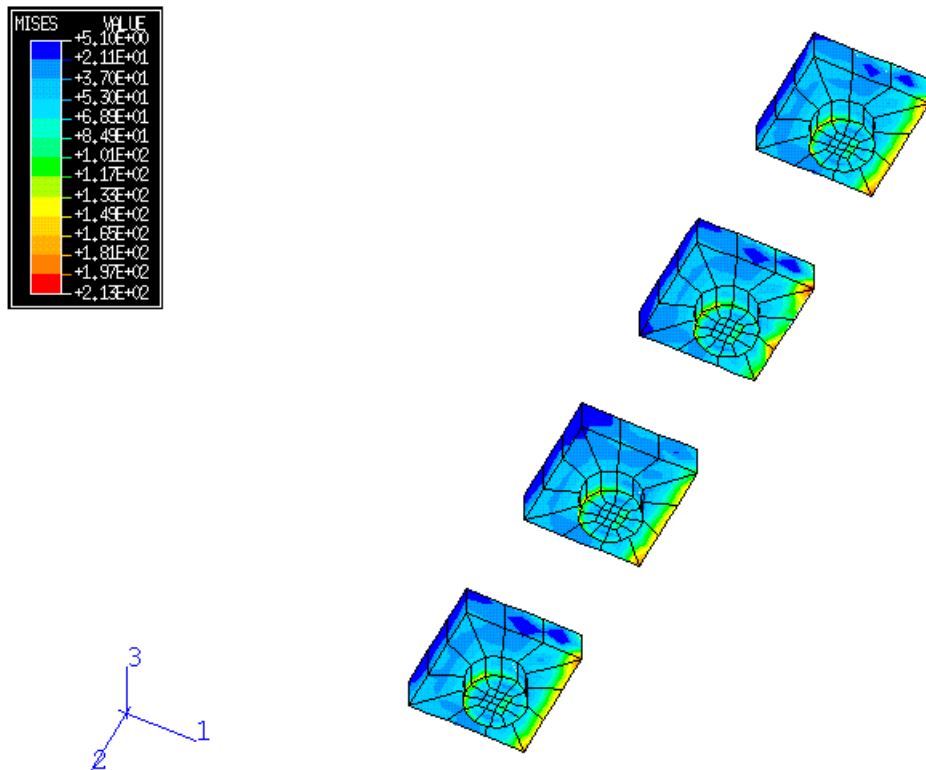


Figure 2.21 von Mises Stress Diagram of Each Bolt used for the L5x3x3/8
Double Angle Connection

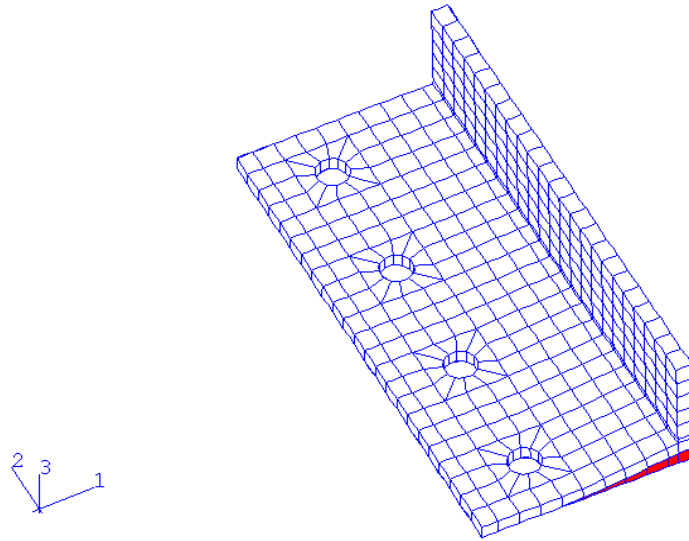
Table 2.6 contains the data for the tension bolt force-applied load relationship of the L5x3x3/8 double angle connection.

Table 2.6 Data for the Tension Bolt Force vs. Applied Load Relationship of the L5x3x3/8 Double Angle Connection

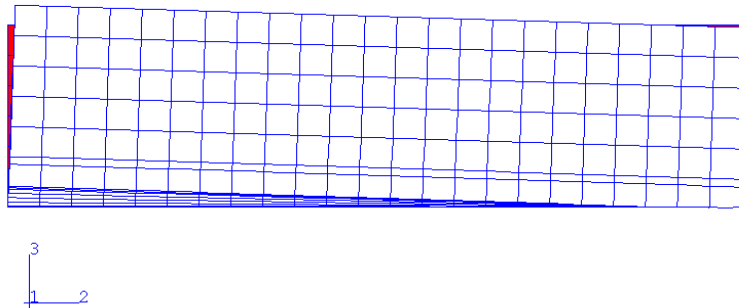
Loading Stage	Applied Load (kips)	Total Bolt Forces (kips)
1	0	112
2	3.72	114.97
3	6.58	116.73
4	10.54	120.05
5	14.83	126.55
6	17.72	133.71
7	18.74	139.40
8	19.33	144.66
9	19.76	148.78
10	20.03	149.83
11	20.23	149.78
12	20.41	149.73
13	20.59	149.68
14	20.74	149.54
15	20.89	149.30
16	21.01	149.09
17	21.13	148.91
18	21.24	148.75
19	21.35	148.60
20	21.43	148.46
21	21.53	148.33

2.2.2.2 Angle Under Shear Loading

An increasing, uniformly distributed load is applied to the beam in the negative Y-direction (downward) as shown in Figure 2.4 to investigate the moment-rotation relationship. Figure 2.22 shows the deformed shape of the angle connection under the applied load of 0.3334kips/in. (total 80 kips). Under the uniformly distributed load, the top of the angle moves in the Z-direction, while the bottom of the angle remains in the same position, restrained by the spring elements. Figure 2.23 presents the moment-rotation relationship of the L5x3x3/8 double angle connection. The moment-rotation curve shows almost a linear relationship after the second loading stage (at the applied load of 0.8 kips) and flattens out as the moment increases. The initial rotational stiffness of the angle connection is approximately 6,119 in.-kips/rad. Table 2.7 contains the data for this moment-rotation relationship of the L5x3x3/8 double angle connection under shear loading.



(a) Deformed Shape of an Angle Model



(b) Side View of a Back-to-Back Angle Leg

Figure 2.22 Deformed Shape of an L5x3x3/8 Double Angle Connection
due to Shear Loading

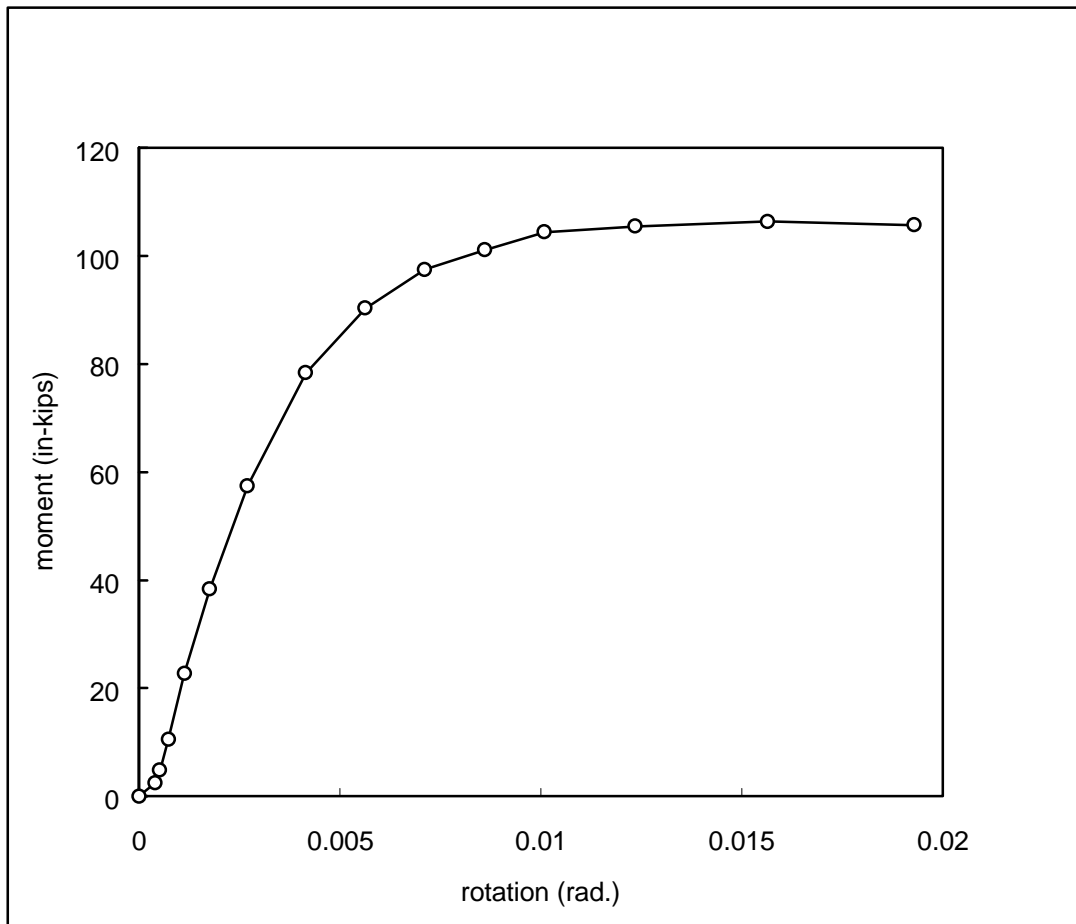


Figure 2.23 Moment-Rotation Relationship of an L5x3x3/8 Double Angle Connection
due to Shear Loading

Table 2.7 Data for the Moment-Rotation Relationship of an L5x3x3/8 Double Angle

Connection due to Shear Loading

Loading Stage	Applied Load (kips)	Rotation (rad.)	Moment (in.-kips)
1	0	0	0
2	0.8	0.0004	2.51
3	1.6	0.0005	4.78
4	2.84	0.0007	10.52
5	4.75	0.0011	22.73
6	7.57	0.0018	38.36
7	11.71	0.0027	57.48
8	17.74	0.0042	78.39
9	23.59	0.0056	90.31
10	29.33	0.0071	97.50
11	35.01	0.0086	101.13
12	40.66	0.0101	104.42
13	49.07	0.0124	105.49
14	61.61	0.0157	106.36

Figure 2.24 shows the von Mises stress diagram of an L5x3x3/8 angle at the applied load of 80.2 kips. The yielding zones are formed along the corner of the angle in addition to the top areas of the angle.

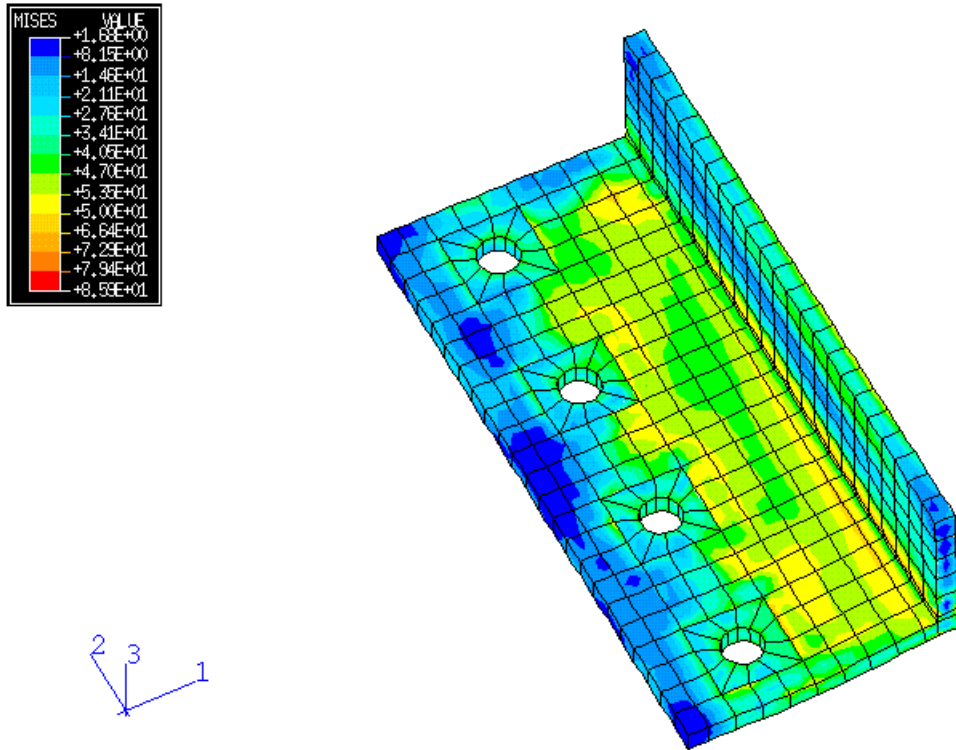


Figure 2.24 von Mises Stress Diagram of an L5x3x3/8 Angle due to Shear Loading

Figure 2.25 presents the von Mises stress diagram of each bolt at the final loading stage. Yielding zones are not formed in the same ways in each bolt indicating that the top areas of the angle are under tension, while the bottom areas of the angle are in compression.

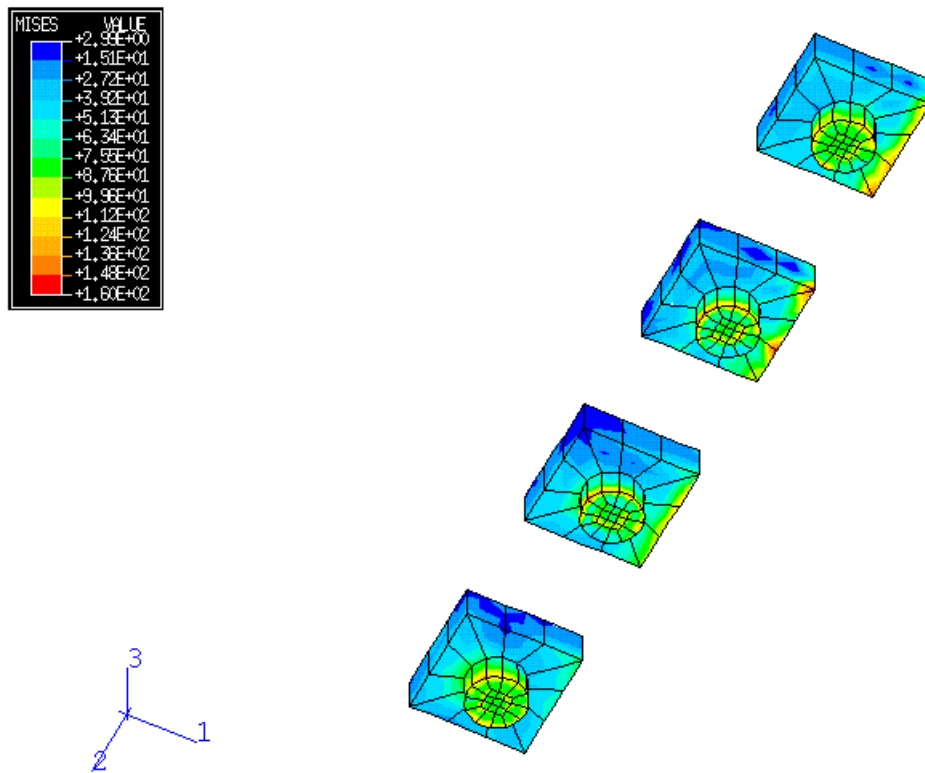
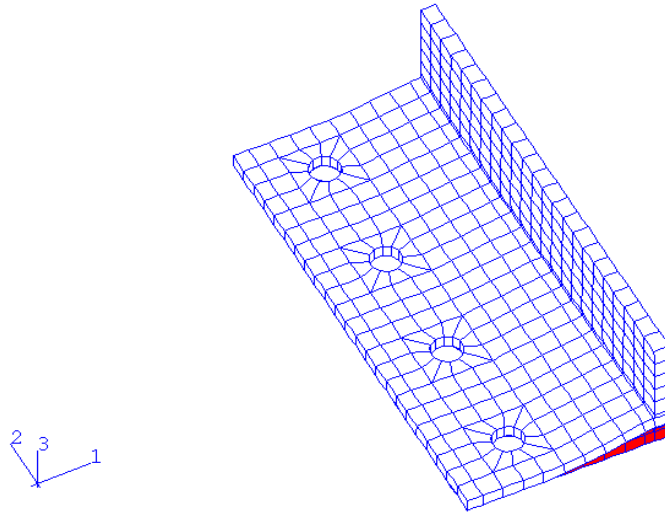


Figure 2.25 von Mises Stress Diagram of Each Bolt used for the L5x3x3/8

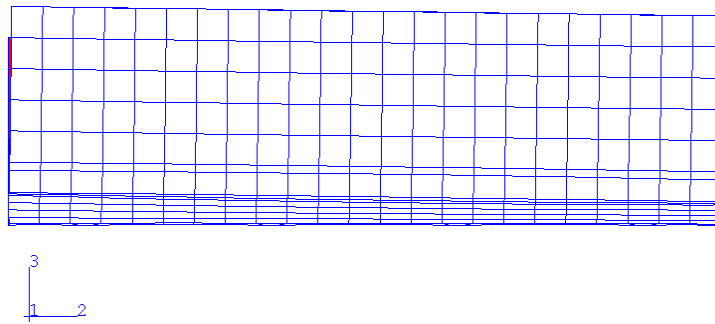
Double Angle Connection

2.2.2.3 Angle Under Axial Tensile Loading Plus Shear Loading

An increasing uniformly distributed load and an increasing axial tensile load are applied to the beam as shown in Figure 2.4 to investigate the moment-rotation relationship of an L5x3x3/8 double angle connection. Figure 2.26 shows the deformed shape of the angle connection under the applied shear load of 0.1961 kips/in. (total 47.1 kips) plus the applied axial tensile load of 1.3295 kips/in. (total 23.5 kips). Under the uniformly distributed load plus the axial tensile load, the top of the angle moves farther in the Z-direction than the bottom of the angle. Figure 2.27 presents the moment-rotation relationship of the L5x3x3/8 double angle connection. The moment-rotation relationship curve shows almost a linear relationship after the second loading stage (at the applied shear load of 0.8 kips plus the applied tensile load of 0.4 kips). The initial rotational stiffness of the angle connection is approximately 6,795.5 in.-kips/rad. Table 2.8 contains the data for this moment-rotation relationship of an L5x3x3/8 double angle connection under the shear loading plus the axial tensile loading.



(a) Deformed Shape of an Angle Model



(b) Side View of a Back-to-Back Angle Leg

Figure 2.26 Deformed Shape of an L5x3x3/8 Double Angle Connection
due to Axial Tensile Loading plus Shear Loading

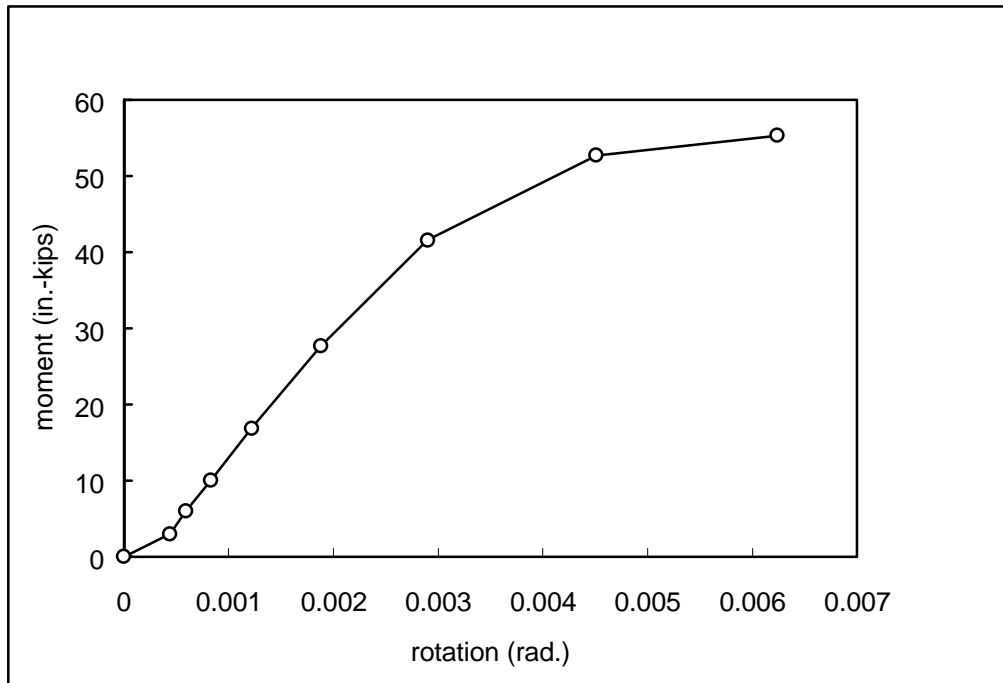


Figure 2.27 Moment-Rotation Relationship of an L5x3x3/8 Double Angle Connection due to Shear Loading plus Axial Tensile Loading

Table 2.8 Data for the Moment-Rotation Relationship of an L5x3x3/8 Double Angle Connection due to Shear Loading plus Axial Tensile Loading

Loading Stage	Q (kips/in.)	T (kips/in.)	Rotation (rad.)	Moment (in.-kips)
1	0	0	0	0
2	0.0033	0.0226	0.0004	2.99
3	0.0067	0.0451	0.0006	5.98
4	0.0116	0.0789	0.0008	10.04
5	0.0191	0.1294	0.0012	16.85
6	0.0303	0.2055	0.0019	27.66
7	0.0469	0.3180	0.0029	41.53
8	0.0710	0.4812	0.0045	52.69
9	0.0942	0.6386	0.0062	55.31

Figure 2.28 shows the von Mises stress diagram of an L5x3x3/8 angle at the applied shear load of 0.1961 kips/in. (total 47.1 kips) plus the applied axial tensile load of 1.3295 kips/in. (total 23.5 kips). Yielding zones are formed in the outstanding leg of the angle near the bolt head and close to the corner of the angle.

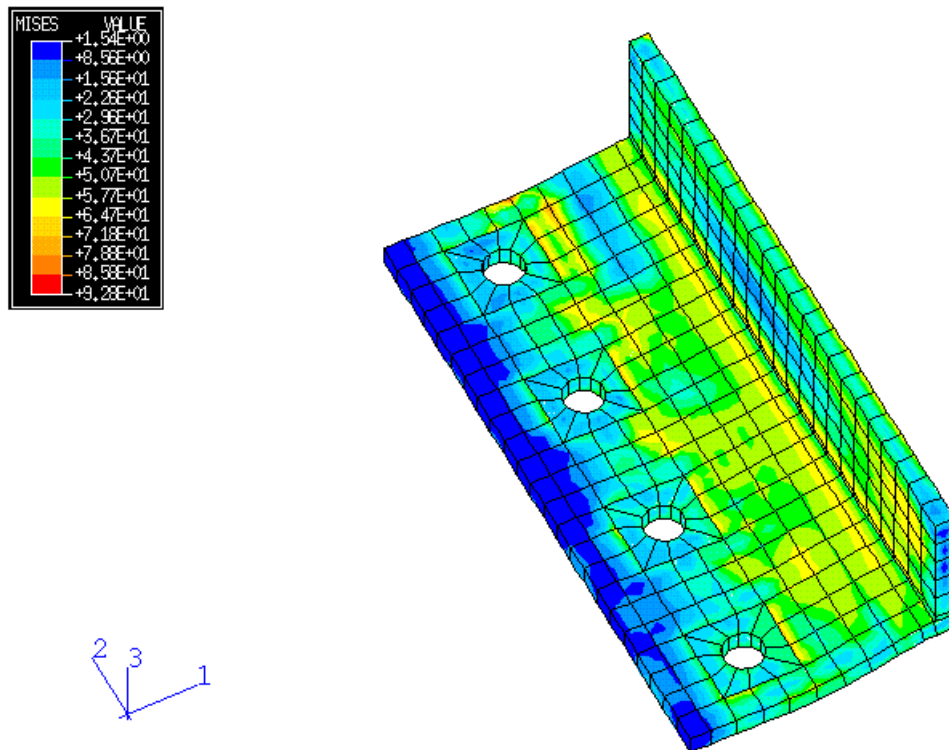
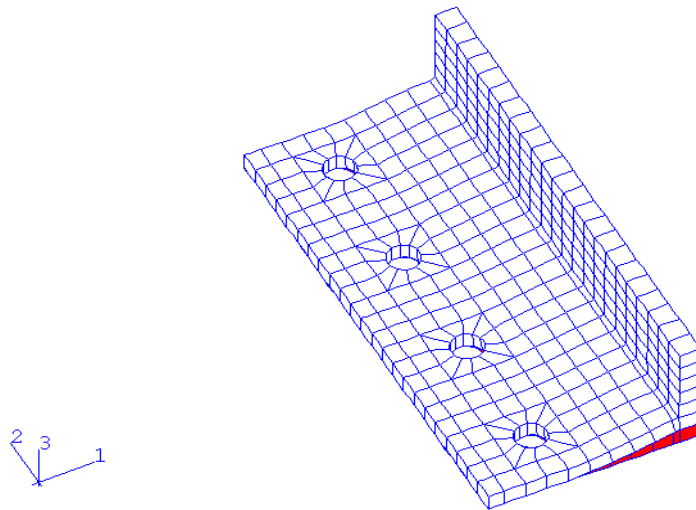


Figure 2.28 von Mises Stress Diagram of an L5x3x3/8 Angle due to Shear Loading plus Axial Tensile Loading

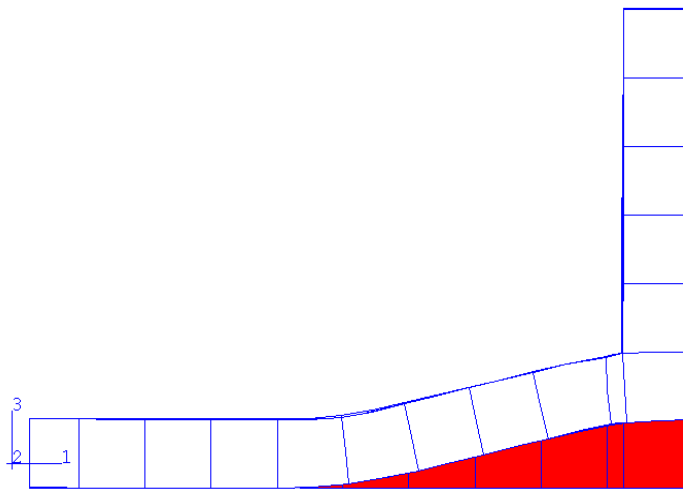
2.2.3 L5x3x1/2 Angle Model

2.2.3.1 Angle Under Axial Tensile Loading

The load-displacement relationship of this angle model was obtained by increasing the load to 2.26 kips/in. (total 40kips) at one end of the beam in the positive Z-direction. Figure 2.29 shows the deformed shape of the angle connection at the applied tensile load of 40 kips. Figure 2.30 presents the load-displacement relationship of an L5x3x1/2 double angle connection. The load-displacement curve shows a linear relationship initially, followed by a rapid decrease in stiffness like the previous load-displacement curves. The initial stiffness of this angle model is 1,013 kips/in., while the final stiffness is approximately 6.8 kips/in. Table 2.9 contains the above load-displacement relationship at each loading stage.



(a) Deformed Shape of an Angle Model



(b) Side View of a Deformed Angle Model

Figure 2.29 Deformed Shape of an L5x3x1/2 Double Angle Connection
due to Tension Loading

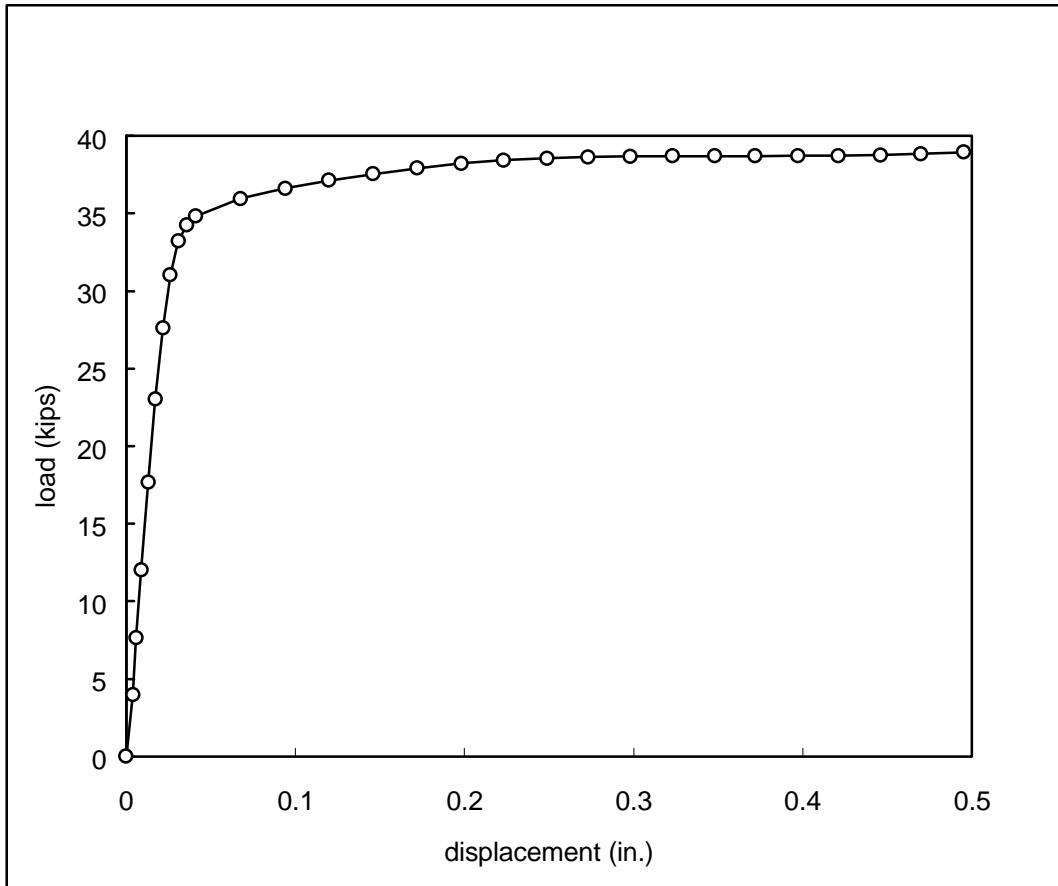


Figure 2.30 Load-Displacement Relationship of an L5x3x1/2 Double Angle Connection due to Tension Loading

Table 2.9 Data for the Load-Displacement Relationship of an L5x3x1/2
 Double Angle Connection due to Tension Loading

Loading Stage	Displacement (in.)	Load (kips)
1	0	0
2	0.004	3.97
3	0.006	7.64
4	0.009	12.04
5	0.013	17.66
6	0.017	23.05
7	0.022	27.60
8	0.026	31.06
9	0.031	33.23
10	0.036	34.26
11	0.041	34.81
12	0.068	35.96
13	0.094	36.61
14	0.120	37.13
15	0.146	37.55
16	0.172	37.92
17	0.198	38.22
18	0.223	38.44
19	0.249	38.56
20	0.273	38.64
21	0.298	38.68
22	0.323	38.70
23	0.348	38.70
24	0.372	38.70
25	0.397	38.71
26	0.421	38.72
27	0.446	38.77
28	0.470	38.84
29	0.495	38.95

Figure 2.31 shows the von Mises stress diagram of the L5x3x1/2 angle specimen at the final loading stage. Yielding zones are formed in the outstanding leg of the angle near the bolt heads and close to the corner of the angle. Yielding zones are also formed near the center of each bolt hole area. The stress fields are more widely spread than in the previous two cases.

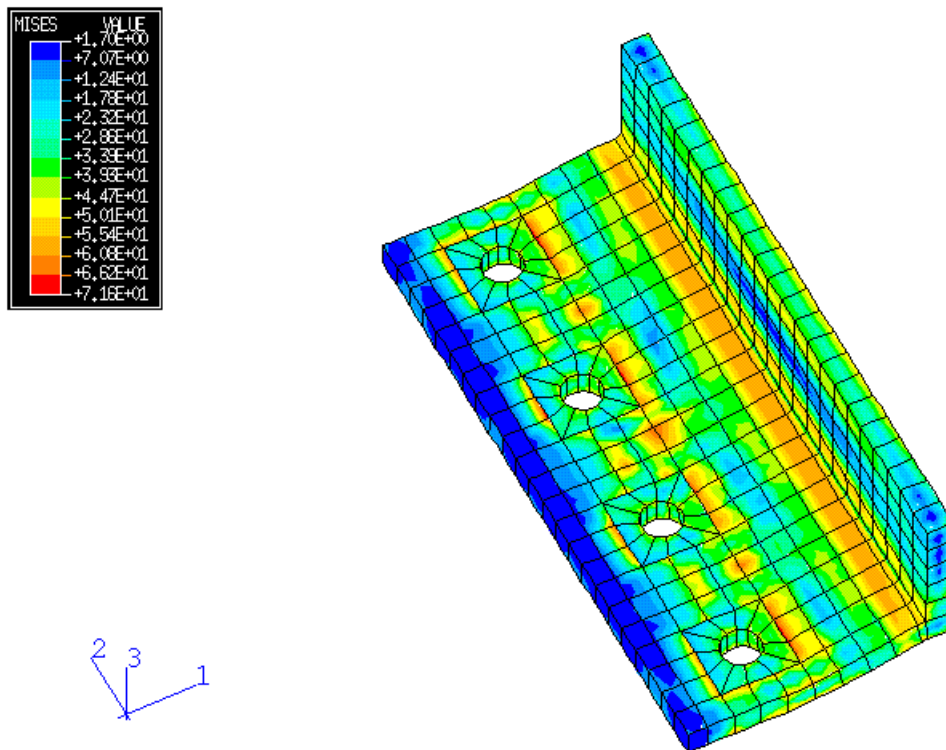


Figure 2.31 von Mises Stress Diagram of an L5x3x1/2 Angle due to Tension Loading

Figure 2.32 shows the tension bolt force-applied load relationship for the L5x3x1/2 double angle connection. At the applied load of 3.97 kips, the sum of the bolt forces is 1.78 kips. From the applied load-bolt force curve, it can be easily shown that this curve increases more gradually than those of the previous L5x3x1/4 angle model and L5x3x3/8 angle model.

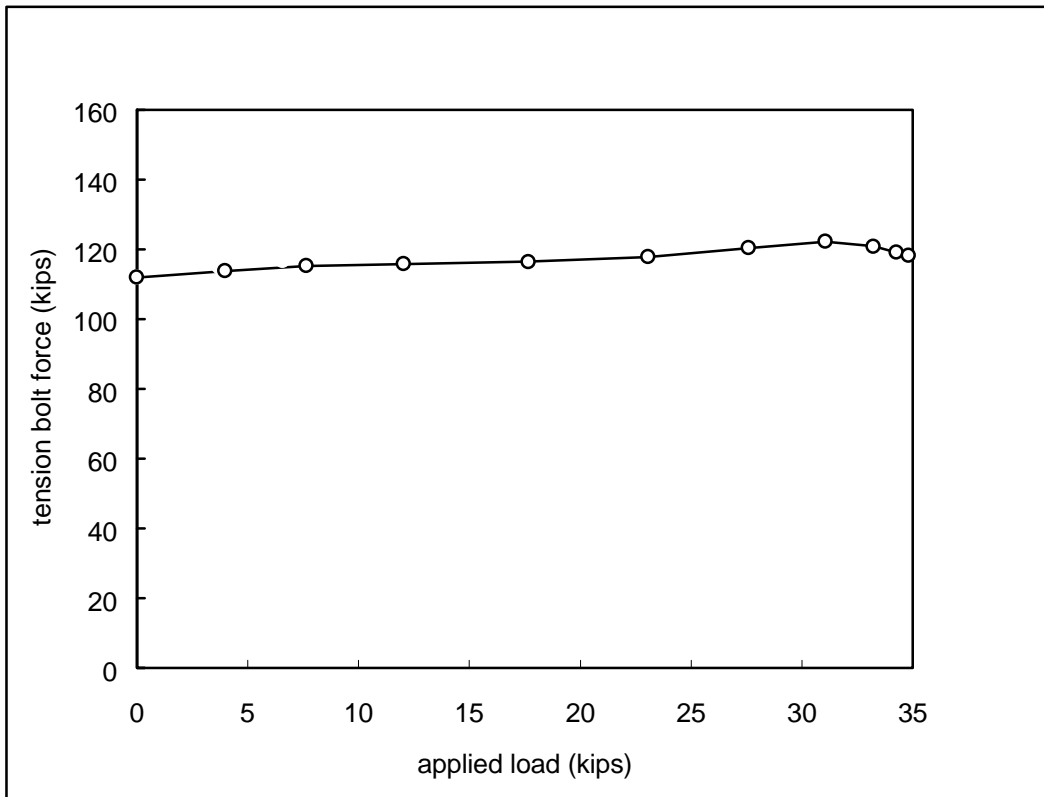


Figure 2.32 Tension Bolt Force vs. Applied Load Relationship of an L5x3x1/2 Double Angle Connection

Figure 2.33 shows the von Mises stress diagram of each bolt at the final loading stage. Fields of high stress are formed in each bolt near the inner edge of the bolt head and outer edge of the bolt shank.

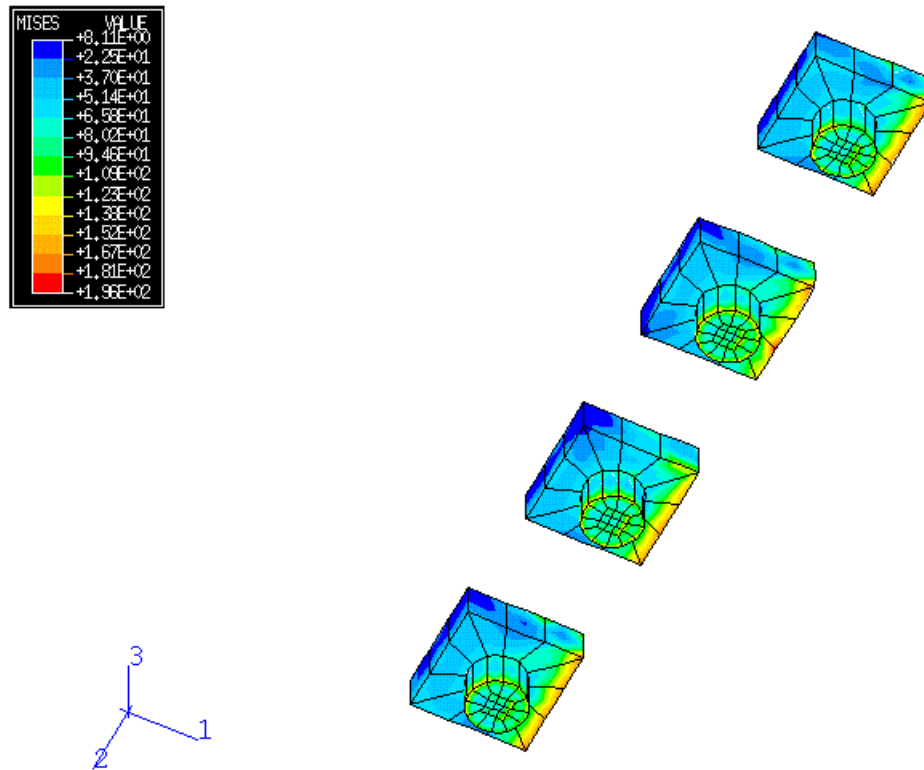


Figure 2.33 von Mises Stress Diagram of Each Bolt used for the L5x3x1/2
Double Angle Connection

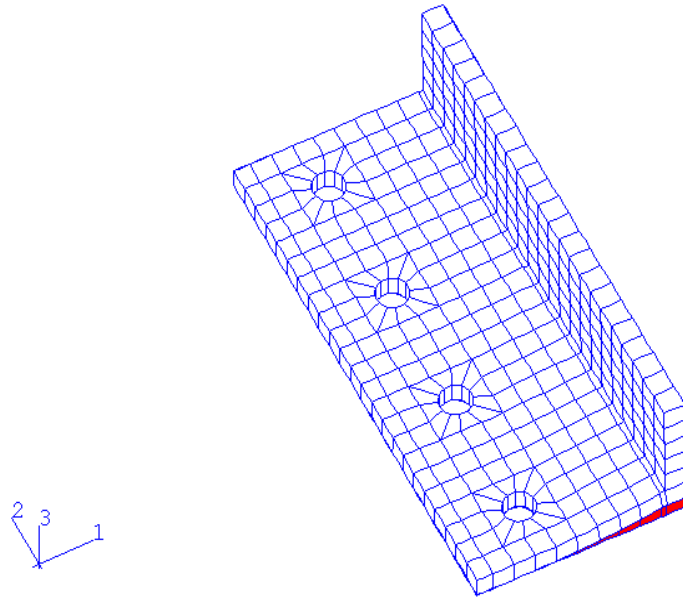
Table 2.10 contains the data for the tension bolt force-applied load relationship of an L5x3x1/2 double angle connection.

Table 2.10 Data for the Tension Bolt Force vs. Applied Load Relationship of an L5x3x1/2 Double Angle Connection

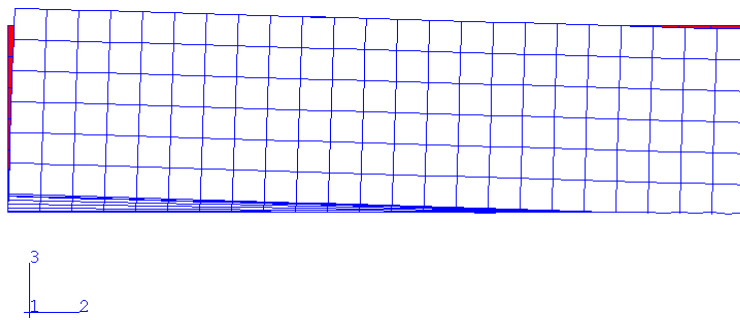
Loading Stage	Applied Load (kips)	Total Bolt Forces (kips)
1	0	112
2	3.97	113.78
3	7.64	115.25
4	12.04	115.79
5	17.66	116.41
6	23.05	117.85
7	27.60	120.39
8	31.06	122.20
9	33.23	120.85
10	34.26	119.15
11	34.81	118.24

2.2.3.2 Angle Under Shear Loading

An increasing, uniformly distributed load up to 0.3334kips/in. (total 80 kips) is applied to a beam element in the negative Y-direction (downward) as shown in Figure 2.4 to investigate the moment-rotation relationship. Figure 2.34 shows the deformed shape of the L5x3x1/2 double angle connection under the maximum applied loads. Under the uniformly distributed load, the top of the angle moves in the positive Z-direction, while the bottom of the angle remains in the same position, resisted by the spring elements. Figure 2.35 presents the moment-rotation relationship of the L5x3x1/2 double angle connection. The moment-rotation curve shows almost a linear relationship after the second loading stage (at the applied load of 0.8 kips) and flattens out as the moment increases. The initial rotational stiffness of the angle connection is approximately 14,606 in.-kips/rad. Table 2.11 contains the data for this moment-rotation relationship of the L5x3x1/2 double angle connection.



(a) Deformed Shape of an Angle Model



(b) Side View of a Back-to-Back Angle Leg

Figure 2.34 Deformed Shape of an L5x3x1/2 Double Angle Connection
due to Shear Loading

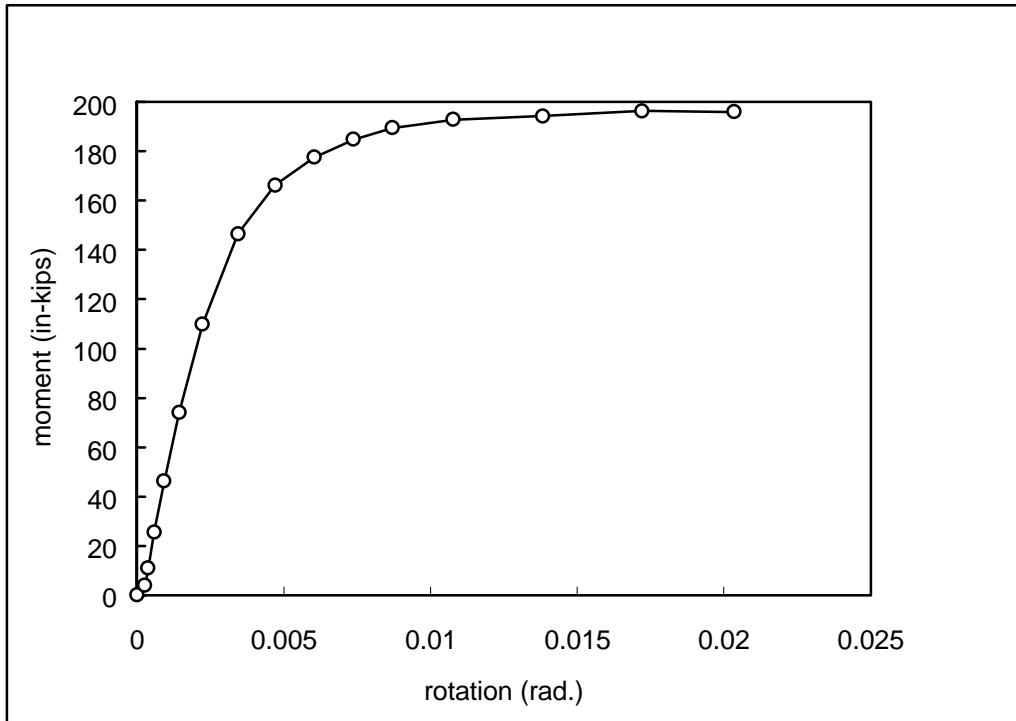


Figure 2.35 Moment-Rotation Relationship of an L5x3x1/2 Double Angle Connection
due to Shear Loading

Table 2.11 Data for the Moment-Rotation Relationship of an L5x3x1/2
 Double Angle Connection due to Shear Loading

Loading Stage	Applied Load (kips)	Rotation (rad.)	Moment (in.-kips)
1	0	0	0
2	0.8	0.00028	4.05
3	1.62	0.00038	10.89
4	2.97	0.00059	25.56
5	4.95	0.00092	46.26
6	7.85	0.00144	73.99
7	12.09	0.00223	109.95
8	18.09	0.00344	146.55
9	23.73	0.00471	166.23
10	29.18	0.00604	177.57
11	34.53	0.00738	184.75
12	39.84	0.00870	189.54
13	47.72	0.01078	192.81
14	59.44	0.01383	194.32
15	70.18	0.01722	196.38

Figure 2.36 shows the von Mises stress diagram of the L5x3x1/2 angle at the applied load of 80.9 kips. Yielding zones are formed along the corner of the angle in addition to the top areas of the angle. Stress fields are also formed around each bolt hole.

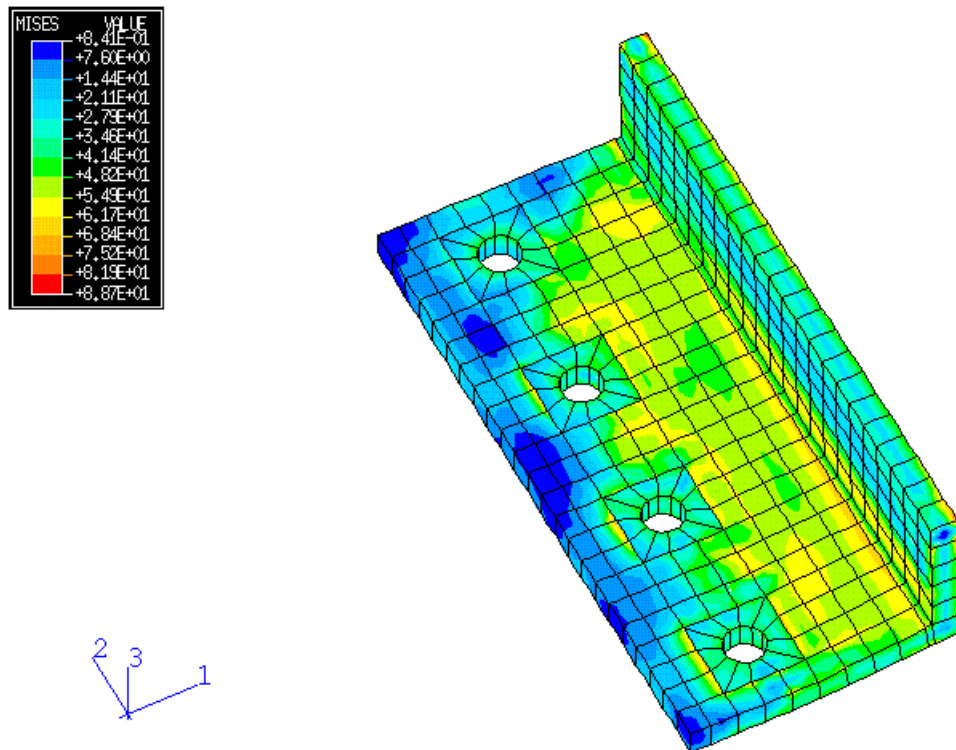


Figure 2.36 von Mises Stress Diagram of an L5x3x1/2 Angle due to Shear Loading

Figure 2.37 presents the von Mises stress diagram of each bolt at the final loading stage. Yielding zones are not formed in the same way in each bolt indicating that the top areas of the angle are under tension, while the bottom areas of the angle are in compression. Fields of high stress are also formed in each bolt shank and at the outer edge of the bolt head.

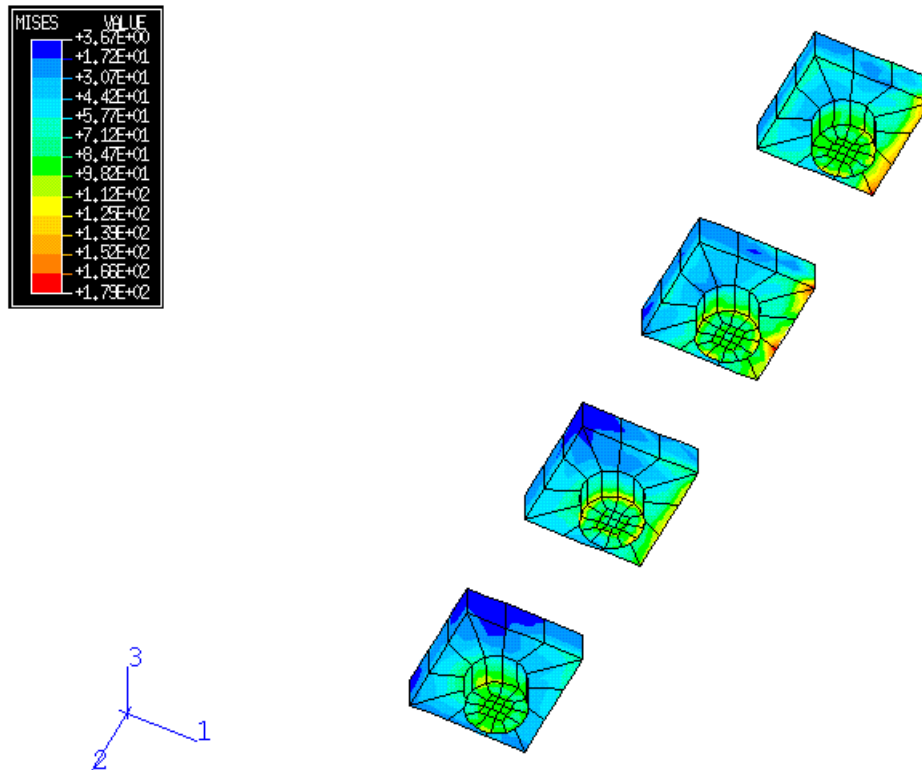
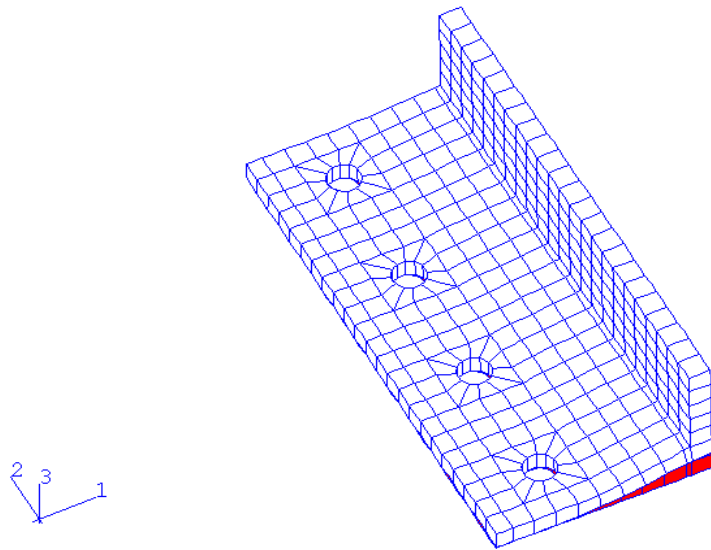


Figure 2.37 von Mises Stress Diagram of Each Bolt used for the L5x3x1/2

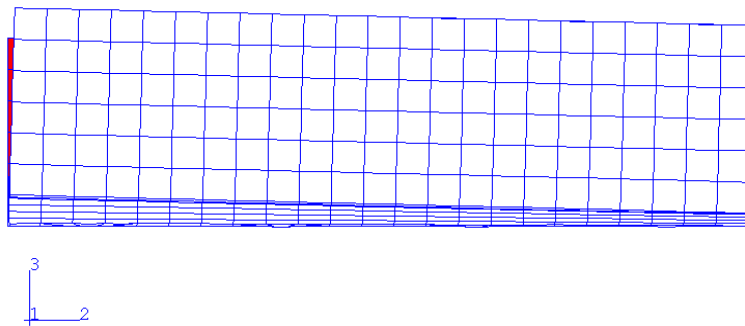
Double Angle Connection

2.2.3.3 Angle Under Axial Tensile Loading Plus Shear Loading

An increasing uniformly distributed load and an increasing axial tensile load are applied to the beam as shown in Figure 2.4 to investigate the moment-rotation relationship of an L5x3x1/2 double angle connection. Figure 2.38 shows the deformed shape of the angle connection under the applied shear load of 0.318 kips/in. (total 76.3 kips) plus the applied axial tensile load of 2.156 kips/in. (total 38.2 kips). Under the uniformly distributed load plus the axial tensile load, the top of the angle moves farther in the Z-direction than the bottom of the angle. Figure 2.39 presents the moment-rotation relationship of the L5x3x1/2 double angle connection. The moment-rotation relationship curve shows a linear relationship initially. The initial rotational stiffness of the angle connection is approximately 43,271 in.-kips/rad. Table 2.12 contains the data for this moment-rotation relationship of an L5x3x1/2 double angle connection under the shear loading plus the axial tensile loading.



(a) Deformed Shape of an Angle Model



(b) Side View of a Back-to-Back Angle Leg

Figure 2.38 Deformed Shape of an L5x3x1/2 Double Angle Connection
due to Axial Tensile Loading plus Shear Loading

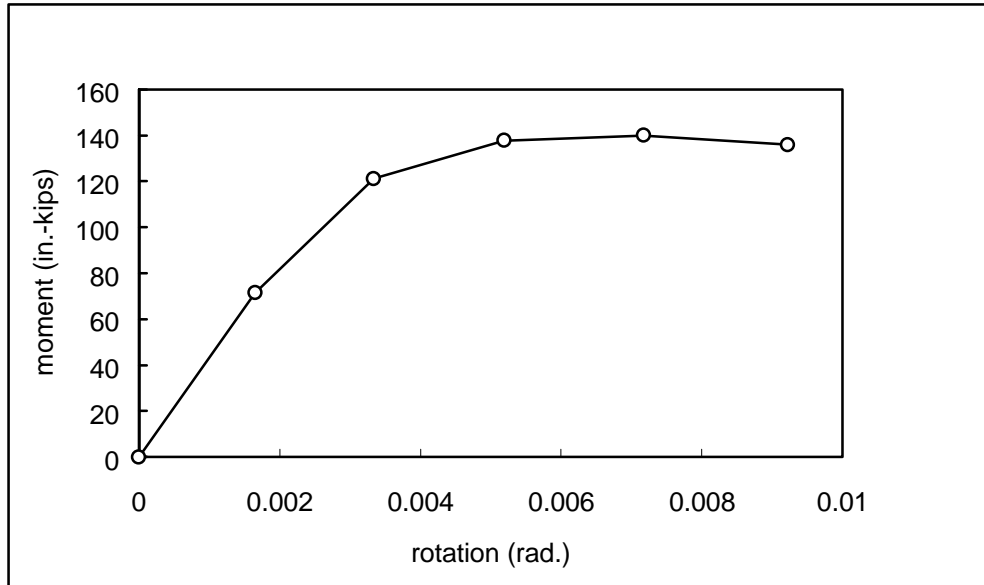


Figure 2.39 Moment-Rotation Relationship of an L5x3x1/2 Double Angle Connection due to Shear Loading plus Axial Tensile Loading

Table 2.12 Data for the Moment-Rotation Relationship of an L5x3x1/2 Double Angle Connection due to Shear Loading plus Axial Tensile Loading

Loading Stage	Q (kips/in.)	T (kips/in.)	Rotation (rad.)	Moment (in.-kips)
1	0	0	0	0
2	0.0347	0.2351	0.0017	71.40
3	0.0674	0.4572	0.0033	121.12
4	0.0973	0.6599	0.0052	137.73
5	0.1260	0.8542	0.0072	139.98
6	0.1542	1.0454	0.0092	135.92

Figure 2.40 shows the von Mises stress diagram of an L5x3x1/2 angle at the applied shear load of 0.318 kips/in. (total 76.3 kips) plus the applied axial tensile load of 2.156 kips/in. (total 38.2 kips). Yielding zones are formed in the outstanding leg of the angle near the bolt head and close to the corner of the angle.

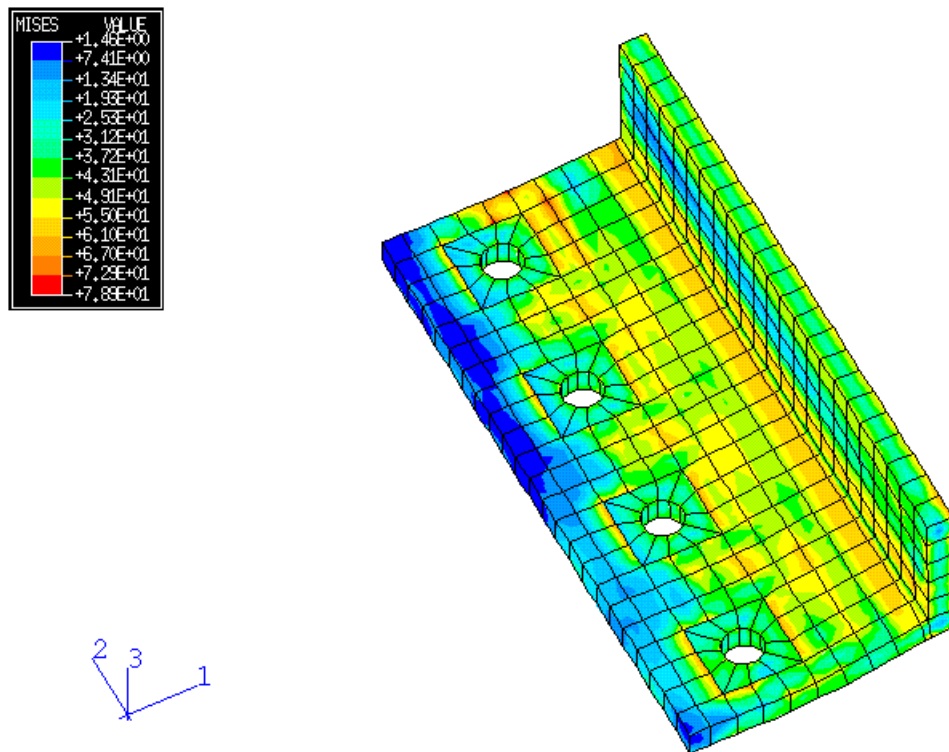


Figure 2.40 von Mises Stress Diagram of an L5x3x1/2 Angle due to Shear Loading plus Axial Tensile Loading

2.3 RICHARD'S FORMULA

2.3.1 Introduction

A finite element model was used to establish double angle connection behavior under axial tensile loads, shear loads, and combined axial tensile loads plus shear loads for three angle sizes. The obtained data is now analyzed by Richard's formula (Richard *et al.* 1988) to obtain the curve sharpness parameter, n , for each case under the given loading conditions. The curve sharpness parameter, n , is an important factor in understanding the behavior of the double angle connection, since it controls the rate of decay of the curve's slope within the given loading conditions. The curve sharpness parameter, n , is also important because it represents physically a measure of imperfections in the connection (Bursi and Leonelli 1994). Richard's formula can be written in the following two forms:

$$R(\Delta) = \frac{(K - K_p)\Delta}{\left(1 + \left|\frac{(K - K_p)\Delta}{R_0}\right|^n\right)^{1/n}} + K_p\Delta \quad (2.1)$$

where,

R =force

D =deformation

K =elastic stiffness

K_p =plastic stiffness

R_0 =reference load

n =curve sharpness parameter

or,

$$M(q) = \frac{(K - K_p)q}{\left(1 + \left|\frac{(K - K_p)q}{M_0}\right|^n\right)^{1/n}} + K_p q \quad (2.2)$$

where,

M = moment

q = rotation

K =elastic rotational stiffness

K_p =plastic rotational stiffness

M_0 =reference moment

n =curve sharpness parameter

The above two formulas provide essentially a good degree of accuracy in approximating the load-displacement relationship or the moment-rotation relationship (Richard *et al.* 1988, Bursi and Leonelli 1994).

2.3.2 Load-Displacement Relationship Under Axial Tensile Loading

Using Richard's formula, the load-displacement curve of the L5x3x1/4 finite element angle model can be approximated with $K=145.5$ kips/in., $K_p =7.6$ kips/in., $R_0 =8.2$ kips, and $n=3.9$. The load-displacement curve of the L5x3x3/8 finite element angle model can be approximated with $K=554.5$ kips/in., $K_p= 9.2$ kips/in., $R_0=19.7$ kips, and $n=4.1$. Similarly, the load-displacement curve of the L5x3x1/2 finite element angle model can be approximated with $K=1,367$ kips/in., $K_p=5.5$ kips/in., $R_0 =36.6$ kips, and $n=4.1$. Figure 2.41 presents the load-displacement relationship for each angle model under axial tensile loads. The load-displacement curves for the 3D finite element models show good

agreement with those of Richard's formula within the given loading range. Table 2.13 is a summary of the Richard's formula parameters for the load-displacement curves.

The load-displacement curve of an equivalent spring model, which will be discussed in Chapter 4, will be plotted based on these Richard's formula parameters. This means that the translational spring stiffness of the equivalent spring model can be obtained from the regression analysis of the load-displacement curve of the 3D finite element model by using Richard's formula.

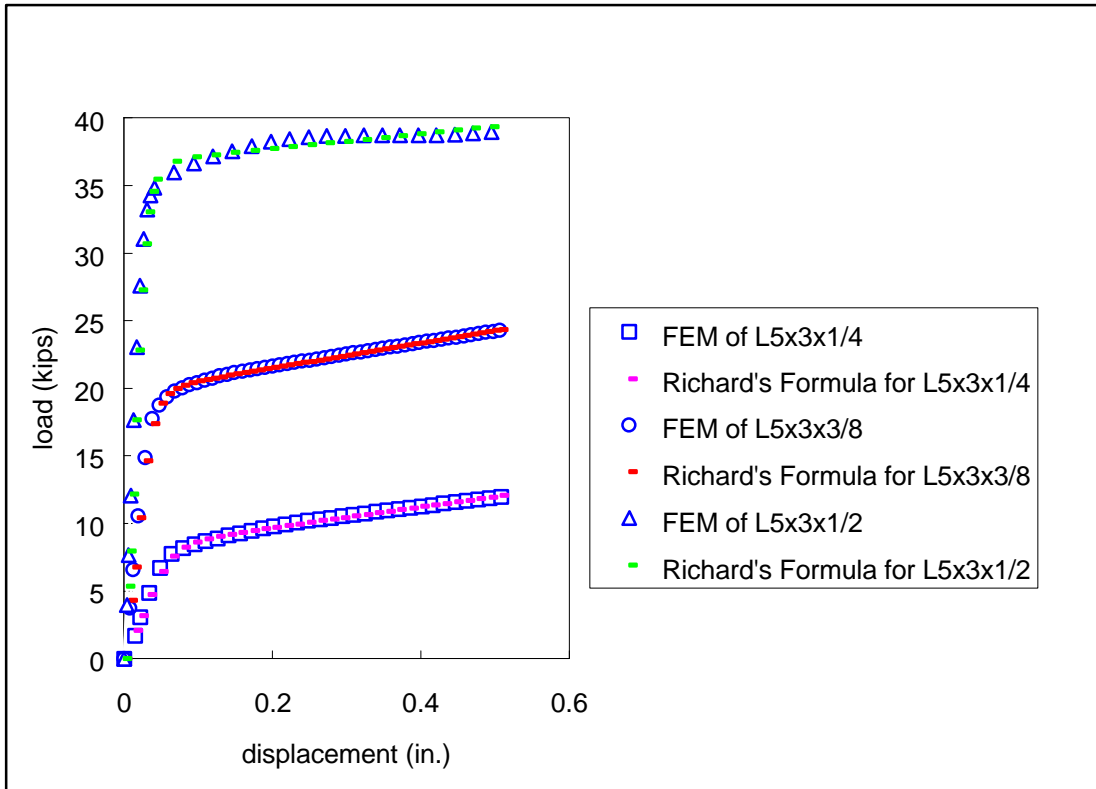


Figure 2.41 Load-Displacement Curves of the 3D Finite Element Models

Table 2.13 Data for the Main Parameters used in Richard's Formula for the Load-Displacement Curves due to Tension Loading

	K (kips/in.)	$K\rho$ (kips/in.)	R_0 (kips)	n
L5x3x1/4 Angle	145.5	7.6	8.2	3.8
L5x3x3/8 Angle	554.5	9.2	19.7	4.1
L5x3x1/2 Angle	1,367	5.5	36.6	4.1

2.3.3 Moment-Rotation Relationship Under Shear Loading

The moment-rotation relationship of a 3D finite element model can be approximated by using Equation 2.2 with regression techniques as mentioned before. The moment-rotation curve of the L5x3x1/4 finite element angle model can be approximated with $K = 5,701$ in.-kips/rad., $K_P = 152.2$ in.-kips/rad., $R_0 = 42.1$ in.-kips, and $n = 5.9$. The moment-rotation curve of the L5x3x3/8 finite element angle model can be approximated with $K=20,757$ in.-kips/rad., $K_P=131$ in.-kips/rad., $R_0=104.2$ in.-kips, and $n=3.7$. Similarly, the moment-rotation curve of the L5x3x1/2 finite element angle model can be approximated with $K=50,383$ in.-kips/rad., $K_P = 432$ in.-kips/rad., $R_0=188.8$ in.-kips, and $n=3.2$. Figure 2.42 shows the moment-rotation relationship of each angle model under shear loads. Even though each regression curve shows an initial discrepancy with that of the finite element angle model, it shows a good agreement after the initial loading stages. Table 2.14 is a summary of the Richard's formula parameters for the moment-rotation curves.

The moment-rotation curve of an equivalent spring model will be plotted based on these Richard's formula parameters. This means that the rotational spring stiffness of the equivalent spring model can be obtained from the regression analysis of the moment-rotation curve of the 3D finite element model by using Richard's formula.

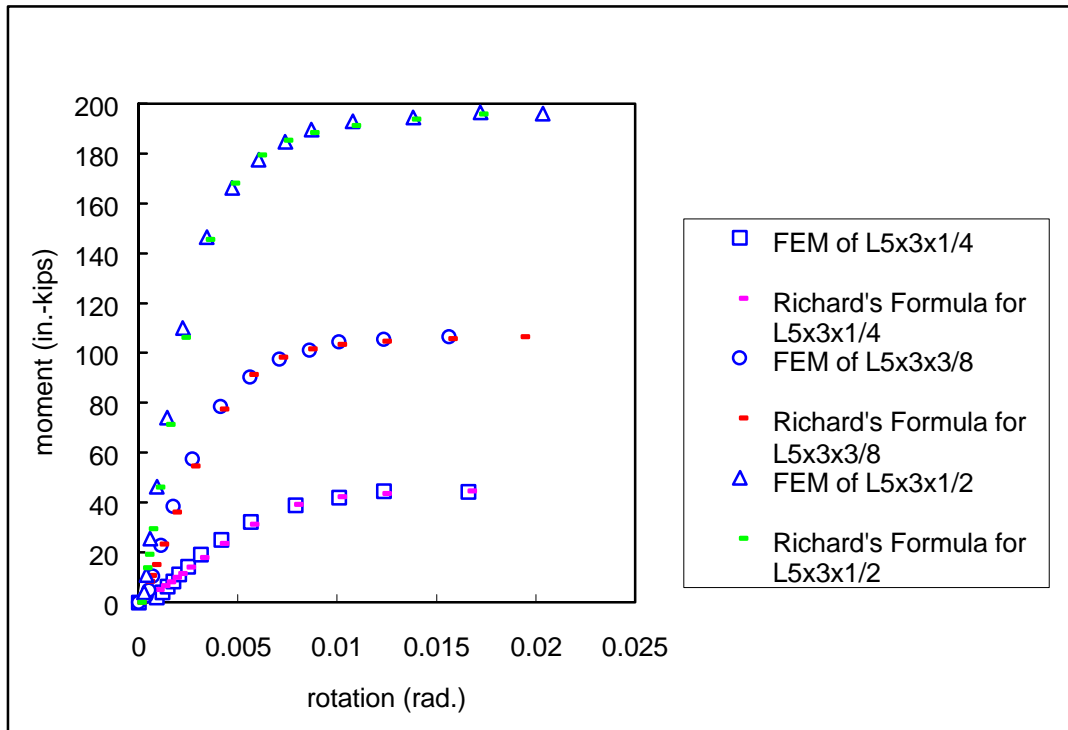


Figure 2.42 Moment-Rotation Curves of the 3D Finite Element Models

Table 2.14 Data for the Main Parameters used in Richard's Formula for the Moment-Rotation Curves due to Shear Loading

	K (in.-kips/rad.)	K_p (in.-kips/rad.)	R_o (in.-kips)	n
L5x3x1/4 Angle	5,701	152.2	42.1	5.9
L5x3x3/8 Angle	20,757	131	104.2	3.7
L5x3x1/2 Angle	50,383	432	188.8	3.2

2.3.4 Moment-Rotation Relationship Under Axial Tensile Loading Plus Shear Loading

To establish the moment-rotation relationship of a 3D finite element model under axial tensile loads plus shear loads, Richard's formula is used with regression techniques. The moment-rotation curve of the L5x3x1/4 finite element angle model can be approximated with $K = 2,869$ in.-kips/rad., $K_p = 124.1$ in.-kips/rad., $R_0 = 13.7$ in.-kips, and $n = 289.6$. The moment-rotation curve of the L5x3x3/8 finite element angle model can be approximated with $K=14,052$ in.-kips/rad., $K_p=1,520$ in.-kips/rad., $R_0=45.8$ in.-kips, and $n=135.6$. Similarly, the moment-rotation curve of the L5x3x1/2 finite element angle model can be approximated with $K=42,402$ in.-kips/rad., $K_p = -354.7$ in.-kips/rad., $R_0=143.5$ in.-kips, and $n=4.6$. Figure 2.43 shows the moment-rotation relationship of each angle model under shear loads. Even though each regression curve shows an initial discrepancy with that of the finite element angle model, it shows a good agreement after the initial loading stages. Table 2.15 is a summary of the Richard's formula parameters for the moment-rotation curves.

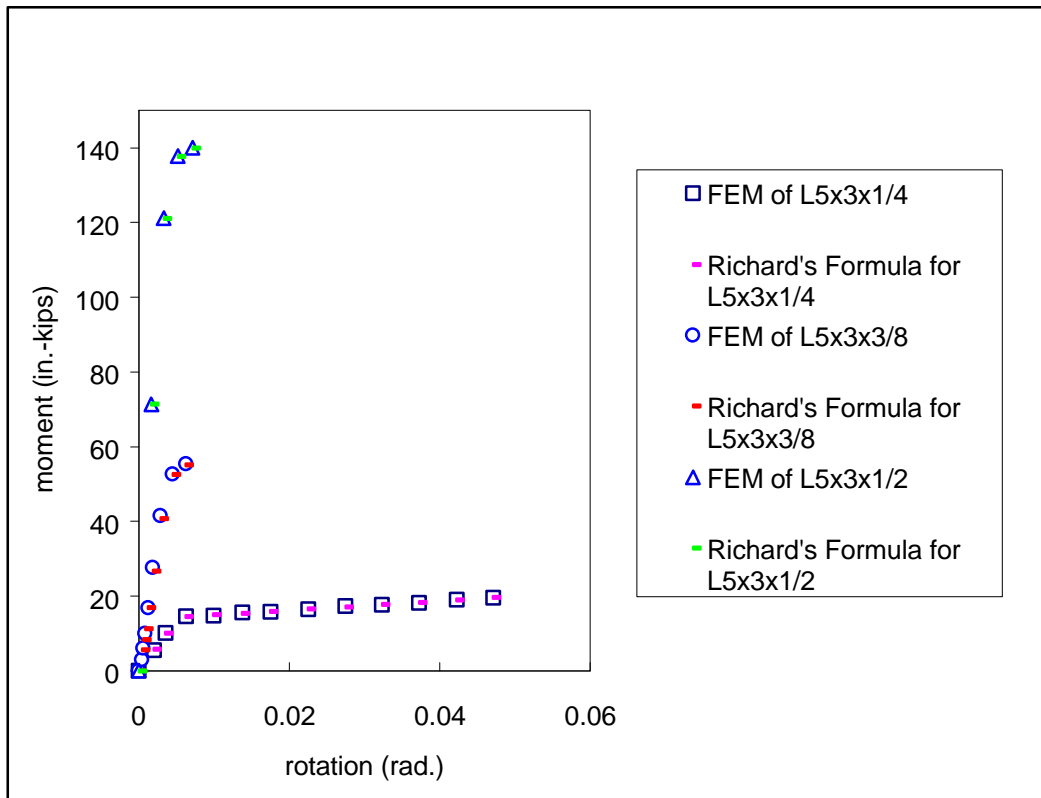


Figure 2.43 Moment-Rotation Curves of 3D Finite Element Models
due to Axial Tensile Loading plus Shear Loading

Table 2.15 Data for the Main Parameters used in Richard's Formula for the
Moment-Rotation Curves due to Shear Loading plus Axial Tensile Loading

	K (in.-kips/rad.)	K_p (in.-kips/rad.)	R_o (in.-kips)	n
L5x3x1/4 Angle	2,869	124.1	13.7	289.6
L5x3x3/8 Angle	14,052	1,520	45.8	135.6
L5x3x1/2 Angle	42,402	-354.7	143.7	4.6

2.4 SUMMARY AND CONCLUSIONS

A 3D nonlinear finite element model has been executed and analyzed to investigate the behavior of double angle connections under axial tensile loads and shear loads, respectively.

From the established load-displacement relationship and the established moment-rotation relationship of the 3D nonlinear finite element model, it can be shown that the angle thickness, t , and the distance, b , play important roles in the initial stiffness, K , of a double angle connection. The parameter, b , defines the distance from the center of a bolt hole to the center line of the back-to-back angle leg of the angle as shown in Figure 2.3. The initial stiffness of a double angle connection is mainly dependent on the value of $(t/b)^3$.

From von Mises stress diagrams, the locations of yielding zones for each case can be shown and they match well with those of yielding zones predicted by Owens and Moore (1992) and Chen and Lui (1991) for double angle connections under axial tensile loads and shear loads, respectively.

To confirm the acceptance of this 3D nonlinear finite element model again, experimental tests were performed for a double angle connection using L5x3x1/4 and L5x3x1/2 angle sections. They are described in the following chapter.